



**Alfred Gessow Rotorcraft Center  
Aerospace Engineering Department  
University of Maryland, College Park**



# **Compact-Reconstruction Weighted Essentially Non-Oscillatory Schemes for Hyperbolic Conservation Laws**

**Debojyoti Ghosh**

**Doctoral Dissertation Defense  
Applied Mathematics & Statistics, and Scientific Computation**

**December 3, 2012  
3164 Martin Hall**

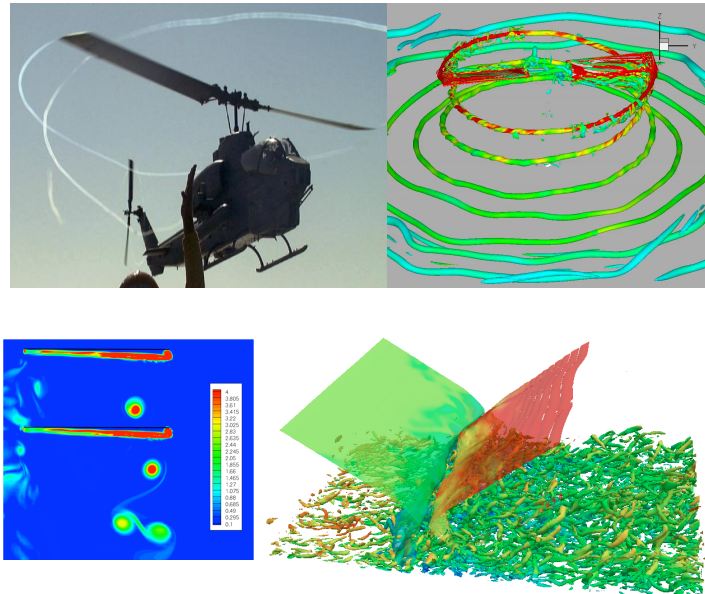
## **Committee**

- Dr. James Baeder (Adviser/Chair)
- Dr. Doron Levy
- Dr. Amir Riaz
- Dr. Anya Jones
- Dr. James Duncan (Dean's Representative)

# Motivation

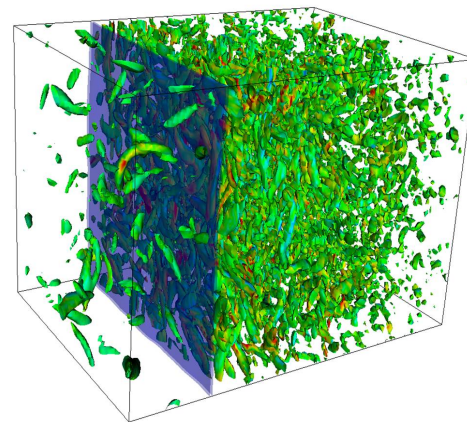
## Numerical Solution of Compressible Turbulent Flows

- Aircraft and Rotorcraft wake flows
- Characterized by **large range of length scales**
- Convection and interaction of eddies
- Compressibility → **Shock waves & Shocklets**
- Thin shear layers → **High gradients** in flow



## High order accurate Navier-Stokes solver

- High spectral resolution for **accurate capturing of smaller length scales**
- Non-oscillatory solution across shock waves and shear layers
- Low dissipation errors for **preservation of flow structures over large distances**





# Outline

- **Hyperbolic Conservation Laws (Introduction / Background)**
  - Numerical solution (Reconstruction + Time – marching)
  - High-resolution schemes in literature (Previous work)
  - Objectives of this thesis
- **Weighted Non – Linear Compact Schemes**
  - Derivation & analysis of 5<sup>th</sup> order Compact-Reconstruction WENO (CRWENO) schemes
  - Application to scalar conservation laws (accuracy, order of convergence, resolution)
  - Numerical cost + computational efficiency (compared to non-compact WENO schemes)
  - Alternative formulations for the non-linear weights
- **Application to the Inviscid Euler Equations**
  - Reconstruction of conserved, primitive and characteristic variables
  - Benchmark 1D and 2D inviscid flow problems (accuracy, convergence, resolution)
  - Numerical cost (conserved/primitive vs. characteristic reconstruction)
- **Integration with a finite volume Navier-Stokes solver**
  - Validation/verification for curvilinear, overset grids with relative motion → Application to flows around airfoils, wings, helicopter rotor blades
  - Direct numerical simulation of compressible, turbulent flows
- **Conclusions and Future Work**



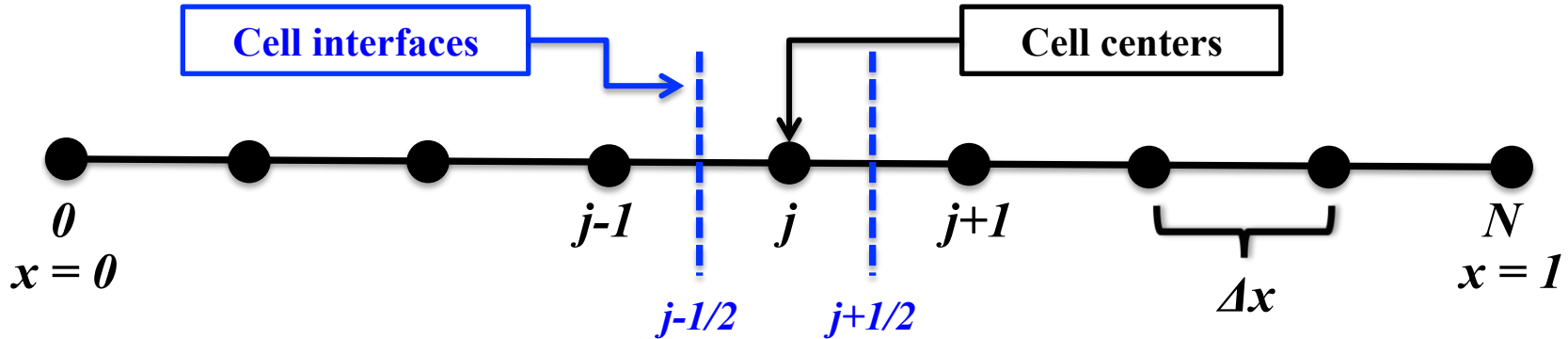
# Introduction / Background



# Hyperbolic Conservation Laws

Scalar hyperbolic partial differential equation

$$u_t + f(u)_x = 0; \quad f'(u) \in \Re$$



Conservative discretization in space leads to an ordinary differential equation in time (solved by explicit / implicit ODE solvers)

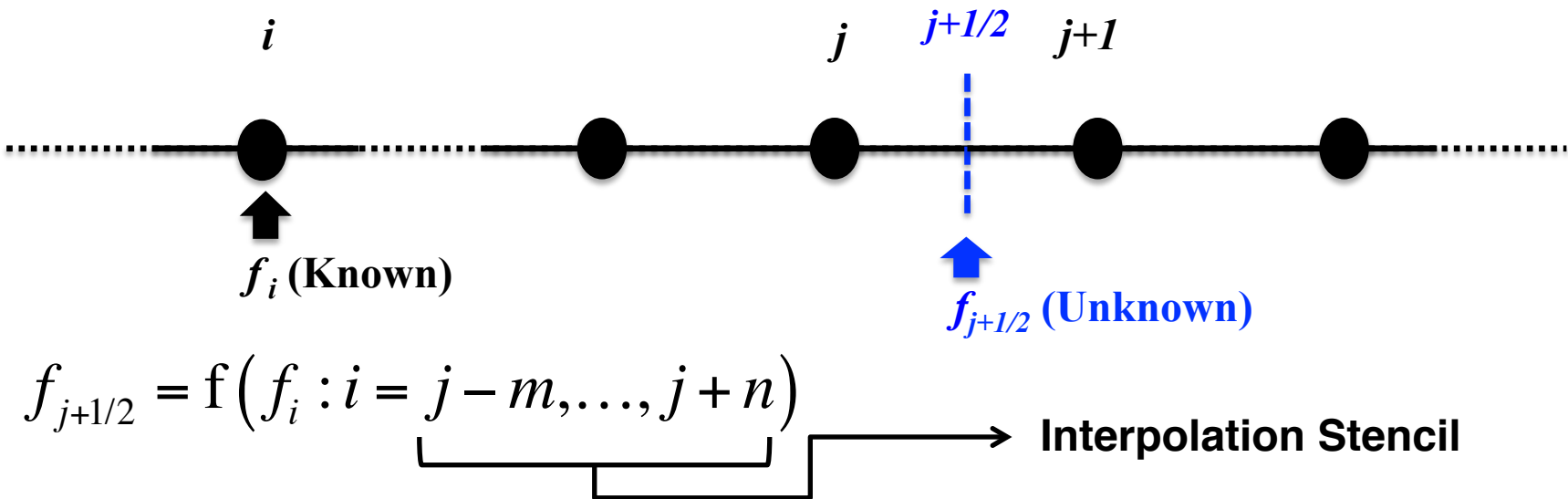
$$\frac{du_j}{dt} + \frac{1}{\Delta x} [f(x_{j+1/2}, t) - f(x_{j-1/2}, t)] = 0$$

Euler Explicit (1<sup>st</sup> order)  
TVD-RK3 (3<sup>rd</sup> order)  
BDF2 (Implicit 2<sup>nd</sup> order)



# Reconstruction of Interface Flux

Reconstruction – interpolation of  $f$  at the interfaces from the cell centered / averaged values (Focus of this thesis)



Upwinding – biased interpolation stencil to model wave nature of the solution

$$f_{j+1/2} = \begin{cases} f_{j+1/2}^L & \text{if } f'(u) \Big|_{x=x_{j+1/2}} > 0; \quad (m \geq n) \\ f_{j+1/2}^R & \text{if } f'(u) \Big|_{x=x_{j+1/2}} < 0; \quad (m < n) \end{cases}$$

Left – biased

Right – biased

# WENO Schemes

## The Weighted Essentially Non-Oscillatory (WENO) schemes

- Liu, Osher & Chan (*JCP*, 1994) and Jiang & Shu (*JCP*, 1996)
- At each interface,  $r$  possible  $r$ -th order interpolation schemes
- Final interface flux = convex combination of the  $r$ -th order interpolations
- Optimal weights in smooth regions →  $(2r-1)$ -th order interpolation
- Smoothness – dependent weights for discontinuous solutions  
→ Non-oscillatory interpolation

$$f_{j+1/2} = \sum_{k=1}^r \omega_k f_{j+1/2}^k$$

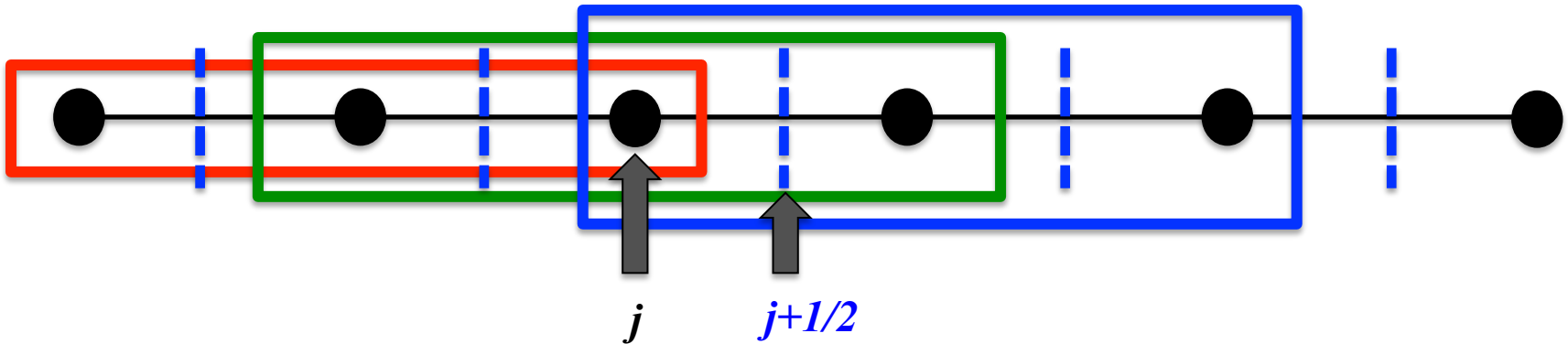
Interface flux  $(2r-1)$ -th order  
 Interface flux  $r$ -th order

$$\alpha_k = \frac{c_k}{(\beta_k + \varepsilon)^p}; \quad \omega_k = \frac{\alpha_k}{\sum_k \alpha_k}$$

Optimal Weights  
 WENO Weights  
 Smoothness Indicators



# 5<sup>th</sup> Order WENO scheme



$$f_{j+1/2} = \frac{1}{3} f_{j-2} - \frac{7}{6} f_{j-1} + \frac{11}{6} f_j$$



$$c_1 = \frac{2}{10} \quad \omega_1$$

$$f_{j+1/2} = -\frac{1}{6} f_{j-1} + \frac{5}{6} f_j + \frac{1}{3} f_{j+1}$$



$$c_2 = \frac{5}{10} \quad \omega_2$$

$$f_{j+3/2} = \frac{1}{3} f_j + \frac{5}{6} f_{j+1} - \frac{1}{6} f_{j+2}$$

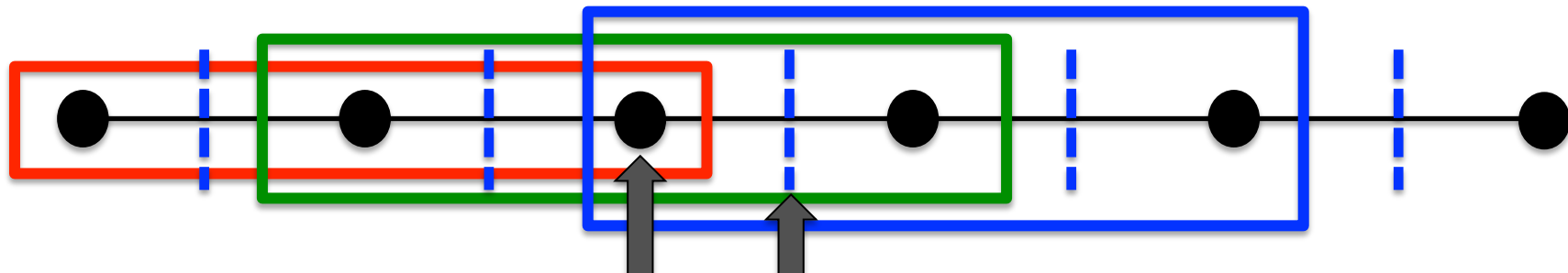


$$c_3 = \frac{3}{10} \quad \omega_3$$

$$f_{j+1/2} = \frac{\omega_1}{3} f_{j-2} - \frac{11}{306} f_j - \frac{13}{60} \omega_1 f_{j-1} + \frac{47}{60} f_{j+1} + \frac{27}{60} \omega_2 f_{j+2} + \frac{1}{20} \omega_3 f_{j+3} + \frac{1}{6} (2\omega_2 + 5\omega_3) f_{j+1} - \frac{\omega_3}{6} f_{j+2}$$

# Non-Linear Weights

Weights are calculated based on smoothness indicators



$$\left. \begin{array}{l} \beta_1 = IS(f_{j-2}, f_{j-1}, f_j) \\ \beta_2 = IS(f_{j-1}, f_j, f_{j+1}) \\ \beta_3 = IS(f_j, f_{j+1}, f_{j+2}) \end{array} \right\} \text{Undivided differences}$$

$$\alpha_k = \begin{cases} \frac{c_k}{(\beta_k + \varepsilon)^p} \\ c_k \left[ 1 + \left( \frac{\tau}{\varepsilon + \beta_k} \right)^p \right] \end{cases}$$

## Implementations of WENO weights:

- Jiang & Shu (1996) → **WENO5-JS**
- Henrick, Aslam & Powers (2005) → **WENO5-M**
- Borges, et. al. (2008) → **WENO5-Z**
- Yamaleev & Carpenter (2009) → **WENO5-YC**



# Compact Difference Schemes

Introduced by Lele (JCP, 1992) in non-conservative form

$$u_t + f(u)_x = 0 \rightarrow \frac{du_j}{dt} + \hat{f}_{x,j} = 0 \quad (\text{Non - conservative discretization})$$

$$\beta \hat{f}_{x,j-2} + \alpha \hat{f}_{x,j-1} + \hat{f}_{x,j} + \alpha \hat{f}_{x,j+1} + \beta \hat{f}_{x,j+2} = a \frac{f_{j+1} - f_{j-1}}{2\Delta x} + b \frac{f_{j+2} - f_{j-2}}{4\Delta x} + c \frac{f_{j+3} - f_{j-3}}{3\Delta x}$$

## Central differencing schemes

$\alpha = \beta = 0$  : Non-compact

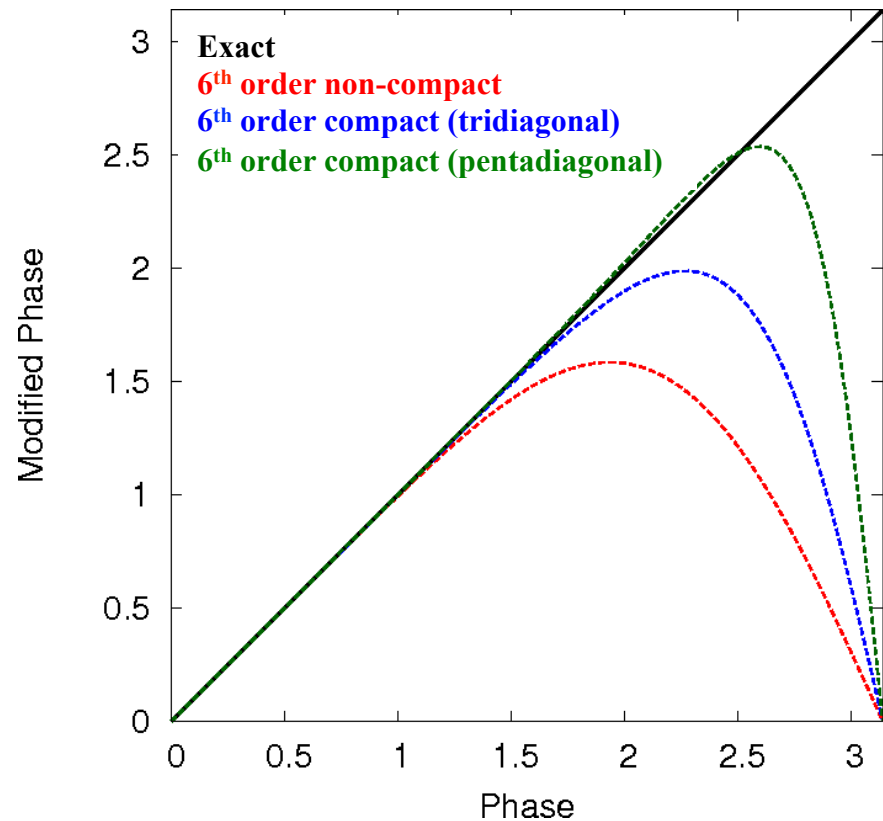
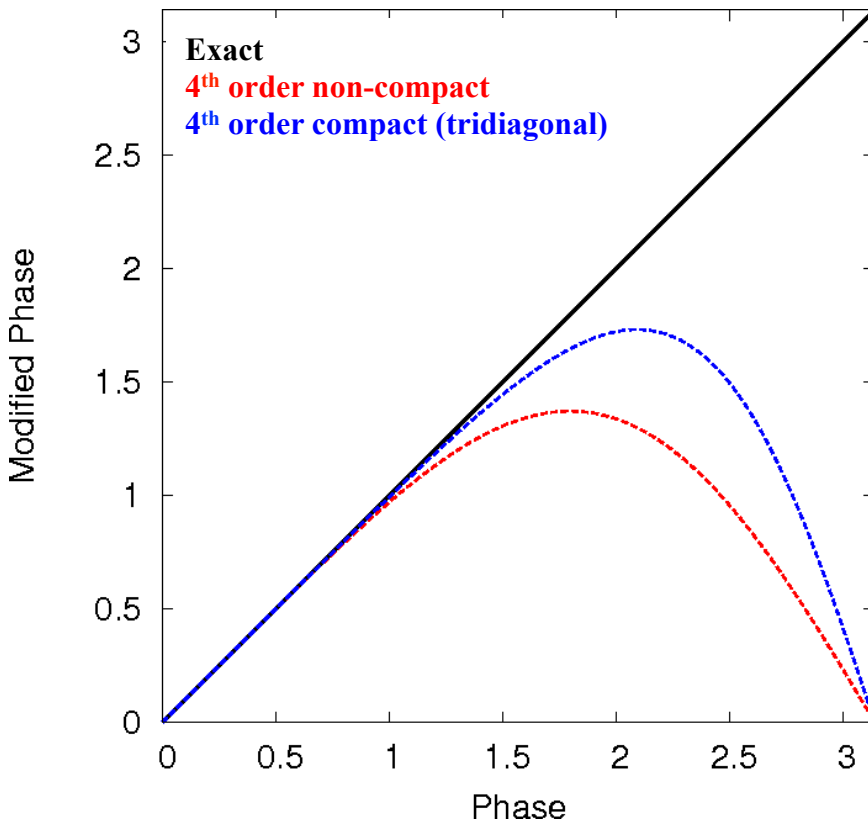
$\beta = 0$  : Tridiagonal compact

$\alpha \neq 0, \beta \neq 0$  : Penta-diagonal compact

- Coupling between neighboring flux derivative approximations
- Requires the **solution of a tridiagonal / penta-diagonal system of equations (sparse LU)**
- Constant coefficients → Pre-computed LU decomposition



# Spectral Resolution of Compact Schemes



Compact schemes have **higher spectral resolution** for same order of convergence → Application to problems with **large range of length scales**

# Previous Work

## Compressible      Turbulent      Flows

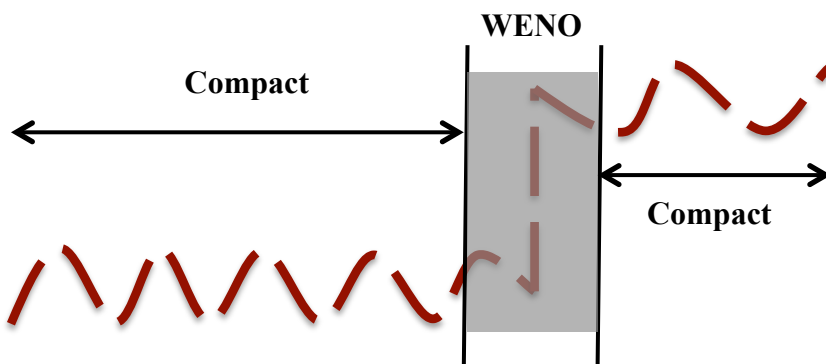
Non-Oscillatory (**WENO Schemes**)



High spectral Resolution (**Compact schemes**)

### Hybrid Compact-WENO Schemes

- Smoothness indicator marks out regions of near discontinuities
- Compact scheme for smooth regions
- WENO scheme near discontinuities
- Adams & Sherriff (1996), Pirozzoli (2002), Ren et. al. (2003)

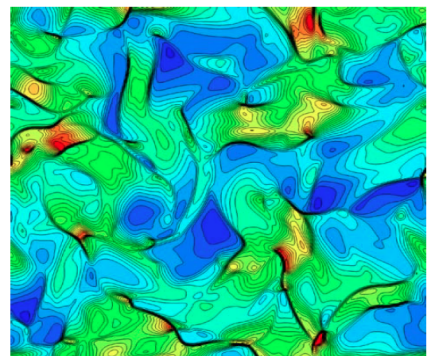


### Disadvantages:

- Loss of spectral resolution near discontinuities
- Requirement of an arbitrary parameter for switching between schemes
- Presence of shocklets throughout the domain → Use

WENO everywhere?

Isotropic Turbulence Decay  
Martin & Taylor, 2007,  
*J. Sci. Comput.*



# Previous Work

## Compressible      Turbulent      Flows

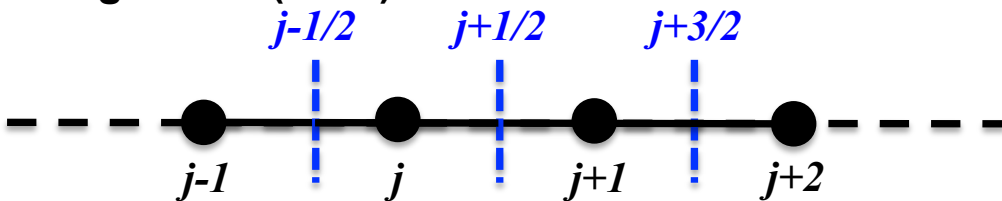
Non-Oscillatory (WENO Schemes)



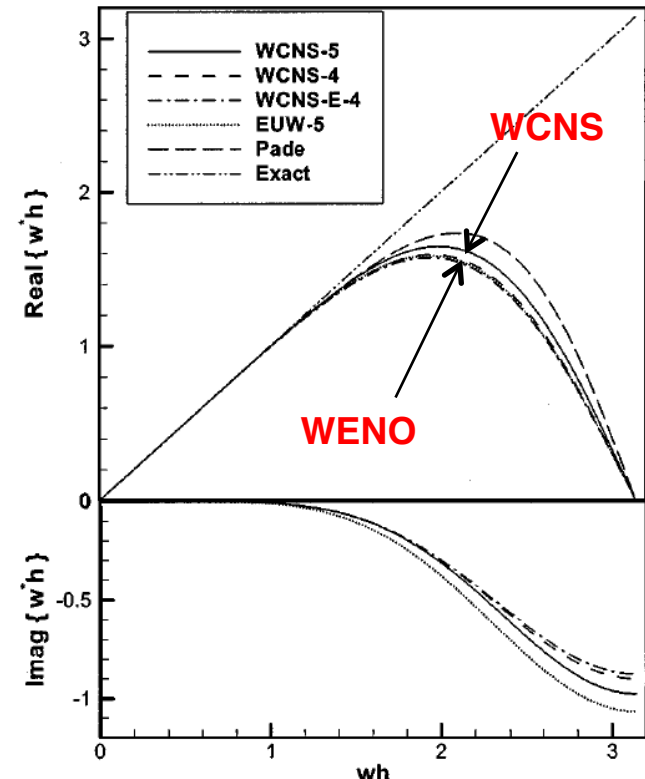
High spectral Resolution (Compact schemes)

### Weighted Compact Non-Linear Schemes (WCNS):

- Non-conservative finite difference discretization for a staggered mesh arrangement
- Step 1:  $f_{j+1/2}$  computed from  $f_j$  using the WENO scheme (Non-oscillatory)
- Step 2:  $f_x$  computed from  $f_{j+1/2}$  using high order central compact difference scheme
- Deng & Zhang (2000), Wang & Huang (2002), Zhang, Jiang & Shu (2008)



Disadvantage: Marginal increase in spectral resolution  
(due to reconstruction of interface flux with WENO scheme)



Deng & Zhang, 2000, J. Comput. Phys.



# Objectives

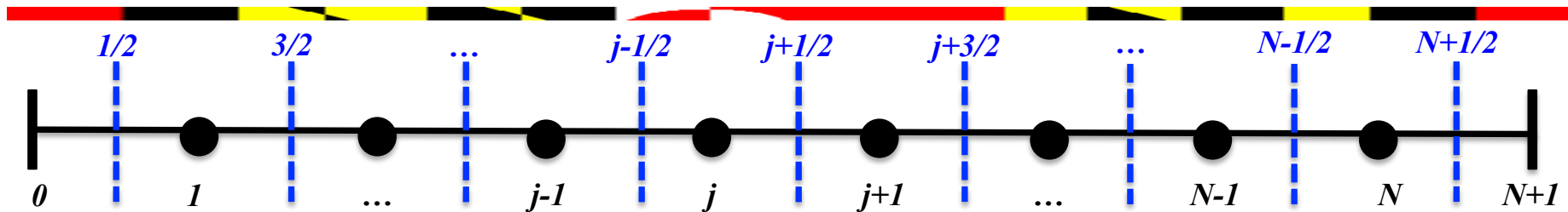
- **Derivation and implementation of CRWENO schemes**
  - Formulation: Identification of lower-order *compact* interpolation schemes & application of WENO weights
  - Numerical analysis of underlying linear schemes
  - Formulation and analysis of boundary closure
  - Application to scalar conservation laws: Study accuracy, convergence, non-oscillatory behavior, and computational efficiency
- **Extension to system of equation: inviscid Euler equations**
  - Application to vector quantities: conserved, primitive & characteristic variables
  - Numerical properties: assessed on benchmark inviscid flow problems
- **Integration with a finite-volume Navier-Stokes solver**
  - Application to steady and unsteady flows around airfoils, wings and rotors: Comparison of the resolution for near-blade and wake flow features
  - Direct numerical simulation of canonical compressible, turbulent flows



# Weighted Non-Linear Compact Schemes



# CRWENO Schemes



- General form of a **conservative compact scheme**:

$$A(\hat{f}_{j+1/2-m}, \dots, \hat{f}_{j+1/2}, \dots, \hat{f}_{j+1/2+m}) = B(f_{j-n}, \dots, f_j, \dots, f_{j+n}) \rightarrow [A]\hat{\mathbf{f}} = [B]\mathbf{f}$$

- At each interface,  $r$  possible  $(r)$ -th order compact interpolations, combined using optimal weights  $c_k$  to yield  $(2r-1)$ -th order compact interpolation scheme:

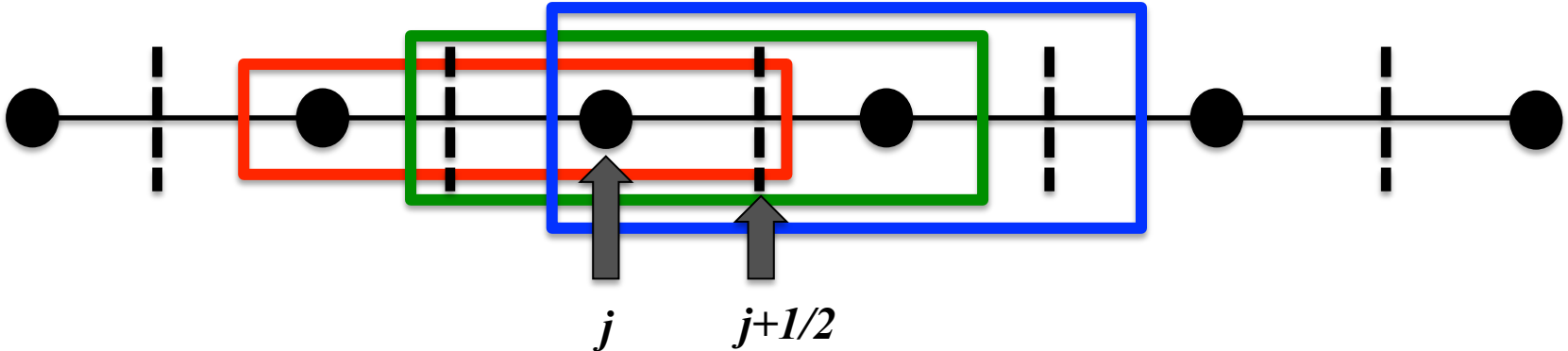
$$\sum_{k=1}^r c_k A_k^r(\hat{f}_{j+1/2-m}, \dots, \hat{f}_{j+1/2+m}) = \sum_{k=1}^r c_k B_k^r(f_{j-n}, \dots, f_{j+n}) \Rightarrow A^{2r-1}(\hat{f}_{j+1/2-m}, \dots, \hat{f}_{j+1/2+m}) = B^{2r-1}(f_{j-n}, \dots, f_{j+n})$$

- Apply **WENO algorithm** on the optimal weights  $c_k$  – scale them according to local smoothness

$$\sum_{k=1}^r \omega_k A_k^r(\hat{f}_{j+1/2-m}, \dots, \hat{f}_{j+1/2+m}) = \sum_{k=1}^r \omega_k B_k^r(f_{j-n}, \dots, f_{j+n}) \quad \alpha_k = \frac{c_k}{(\beta_k + \varepsilon)^p}; \quad \omega_k = \alpha_k / \sum_k \alpha_k$$



# 5<sup>th</sup> Order CRWENO scheme (CRWENO5)



$$\frac{2}{3}f_{j-1/2} + \frac{1}{3}f_{j+1/2} = \frac{1}{6}f_{j-1} + \frac{5}{6}f_j$$



$$c_1 = \frac{2}{10} \quad \omega_1$$

$$\frac{1}{3}f_{j-1/2} + \frac{2}{3}f_{j+1/2} = \frac{5}{6}f_j + \frac{1}{6}f_{j+1}$$



$$c_2 = \frac{5}{10} \quad \omega_2$$

$$\frac{2}{3}f_{j+1/2} + \frac{1}{3}f_{j+3/2} = \frac{1}{6}f_j + \frac{5}{6}f_{j+1}$$



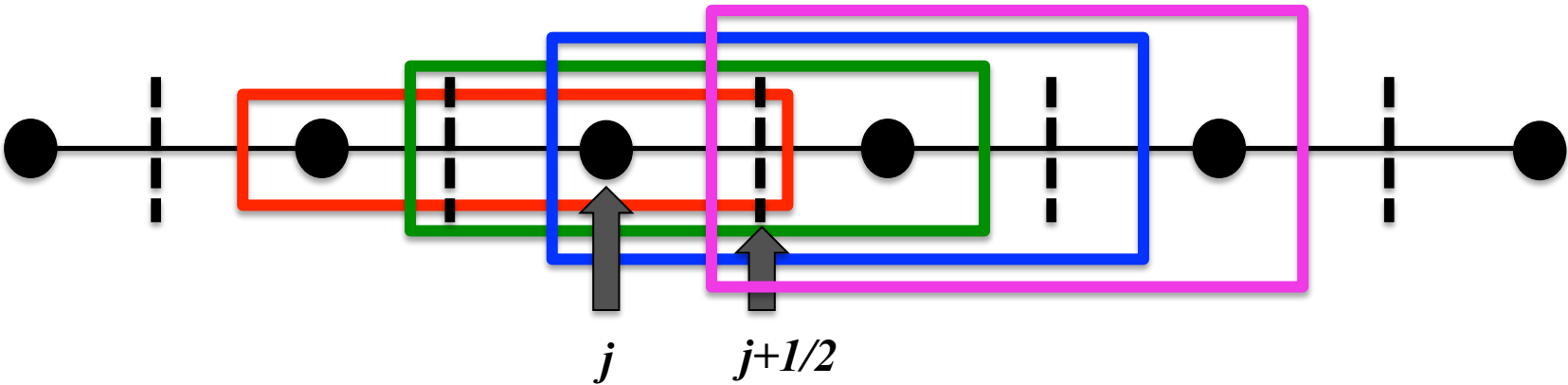
$$c_3 = \frac{3}{10} \quad \omega_3$$

---


$$\left( \frac{2}{3}\omega_1 + \frac{13}{30}\omega_2 f_j f_{j+1/2} + \frac{6}{103}f_j \omega_{1/2} + \frac{2}{3}\left(\omega_2 f_j + \omega_3 f_{j+3/2}\right) \right) \frac{1}{30} f_{j+1/2} f_{j+1}^2 + \frac{19}{30} f_j f_{j+1/2} f_{j+3/2} + \frac{10}{30} f_j f_{j+1} + \frac{5(\omega_1 + \omega_2)}{6} f_j + \frac{\omega_2 + 5\omega_3}{6} f_{j+1}$$



# Low Dissipation 5<sup>th</sup> order CRWENO scheme (CRWENO5-LD)



$$\frac{2}{3}f_{j-1/2} + \frac{1}{3}f_{j+1/2} = \frac{1}{6}f_{j-1} + \frac{5}{6}f_j$$



$$c_1 = \frac{3}{20} \quad \omega_1$$

$$\frac{1}{3}f_{j-1/2} + \frac{2}{3}f_{j+1/2} = \frac{5}{6}f_j + \frac{1}{6}f_{j+1}$$



$$c_2 = \frac{9}{20} \quad \omega_2$$

$$\frac{2}{3}f_{j+1/2} + \frac{1}{3}f_{j+3/2} = \frac{1}{6}f_j + \frac{5}{6}f_{j+1}$$



$$c_3 = \frac{7}{20} \quad \omega_3$$

$$\frac{1}{3}f_{j+1/2} + \frac{2}{3}f_{j+3/2} = \frac{5}{6}f_{j+1} + \frac{1}{6}f_{j+2}$$



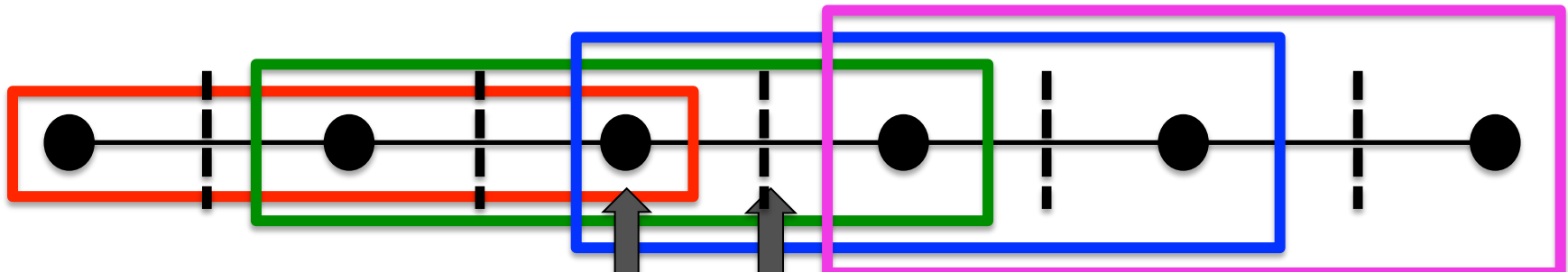
$$c_4 = \frac{1}{20} \quad \omega_4$$

---


$$\left( \frac{2}{3}\omega_1 \frac{5}{20} f_{j+1/2} \right) f_{j+1/2} + \left( \frac{1}{20} \omega_1 \frac{2}{3} (\omega_2 + \frac{3}{20}) f_{j+1/2} \right) f_{j+1/2} - \frac{3}{120} \left( \frac{1}{3} f_{j-1} + \frac{4}{3} \omega_1 f_{j+1/2} \right) f_{j+1/2} + \frac{49}{6120} f_{j+1/2} (\omega_1 + \omega_2) + \frac{1}{6120} f_{j+1/2} \omega_3 f_{j+1} + \frac{\omega_2 + 5(\omega_3 + \omega_4)}{6} f_{j+1} + \frac{\omega_4}{6} f_{j+2}$$

# Smoothness Indicators

Weights are calculated based on smoothness indicators of corresponding explicit stencils (**same as WENO5 scheme**)



$j$        $j+1/2$

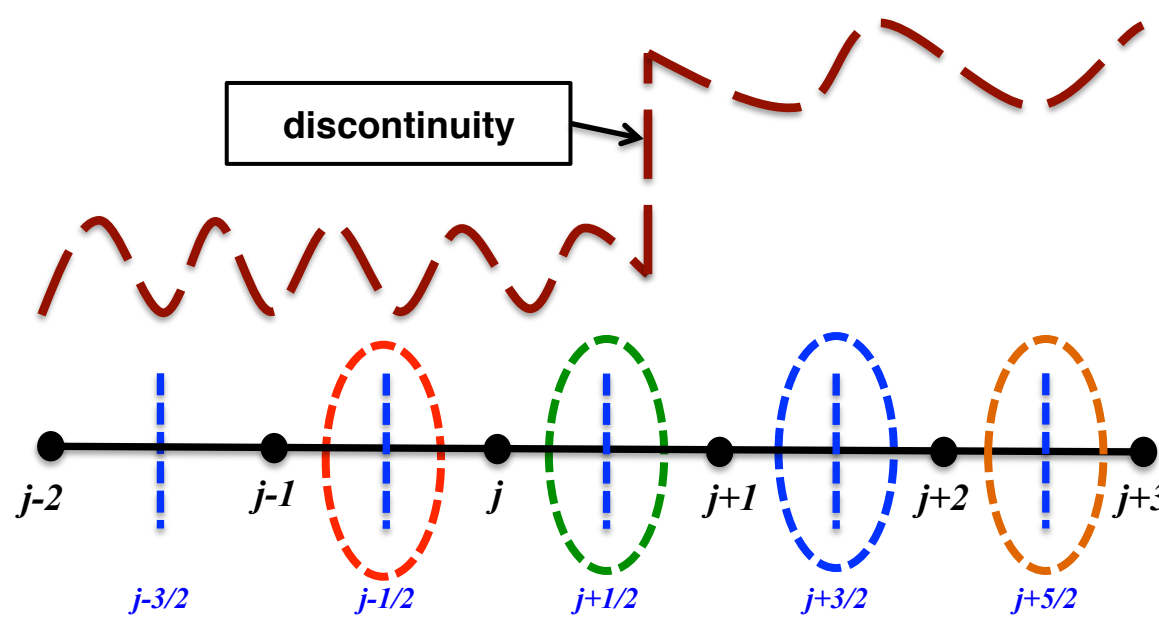
- $\beta_1 = IS(f_{j-2}, f_{j-1}, f_j)$
- $\beta_2 = IS(f_{j-1}, f_j, f_{j+1})$
- $\beta_3 = IS(f_j, f_{j+1}, f_{j+2})$
- $\beta_4 = IS(f_{j+1}, f_{j+2}, f_{j+3})$

$$\alpha_k = \frac{c_k}{(\beta_k + \varepsilon)^p}; \quad \omega_k = \frac{\alpha_k}{\sum_k \alpha_k}; \quad k = 1, 2, 3$$

$$\beta_4 = \max(\beta_3, \beta_4) \text{ (Avoid downwind interpolation)}$$

CRWENO5-LD

# Behavior across Discontinuities



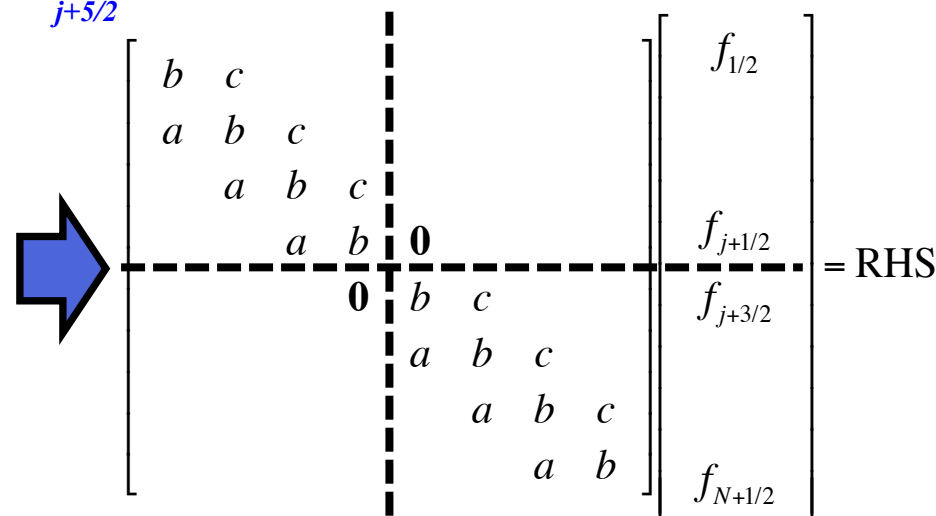
Decoupling of  
domain across  
a discontinuity



$$\frac{2}{3}f_{j-1/2} + \frac{1}{3}f_{j+1/2} = \frac{1}{6}f_{j-1} + \frac{5}{6}f_j \rightarrow \omega_1 \text{ } \color{red}{\times} \color{green}{\times} \color{blue}{0} \color{orange}{0}$$

$$\frac{1}{3}f_{j-1/2} + \frac{2}{3}f_{j+1/2} = \frac{5}{6}f_j + \frac{1}{6}f_{j+1} \rightarrow \omega_2 \text{ } \color{red}{\times} \color{green}{0} \color{blue}{0} \color{orange}{\times}$$

$$\frac{2}{3}f_{j+1/2} + \frac{1}{3}f_{j+3/2} = \frac{1}{6}f_j + \frac{5}{6}f_{j+1} \rightarrow \omega_3 \text{ } \color{red}{0} \color{green}{0} \color{blue}{\times} \color{orange}{\times}$$





# Numerical Analysis

Underlying optimal (**linear**) schemes:

$$f_{j+1/2} = \frac{1}{30}f_{j-2} - \frac{13}{60}f_{j-1} + \frac{47}{60}f_j + \frac{27}{60}f_{j+1} - \frac{1}{20}f_{j+2}$$

**WENO5**

$$\frac{3}{10}f_{j-1/2} + \frac{6}{10}f_{j+1/2} + \frac{1}{10}f_{j+3/2} = \frac{1}{30}f_{j-1} + \frac{19}{30}f_j + \frac{10}{30}f_{j+1}$$

**CRWENO5**

$$\frac{5}{20}f_{j-1/2} + \frac{12}{20}f_{j+1/2} + \frac{3}{20}f_{j+3/2} = \frac{3}{120}f_{j-1} + \frac{67}{120}f_j + \frac{49}{120}f_{j+1} + \frac{1}{120}f_{j+2}$$

**CRWENO5-LD**

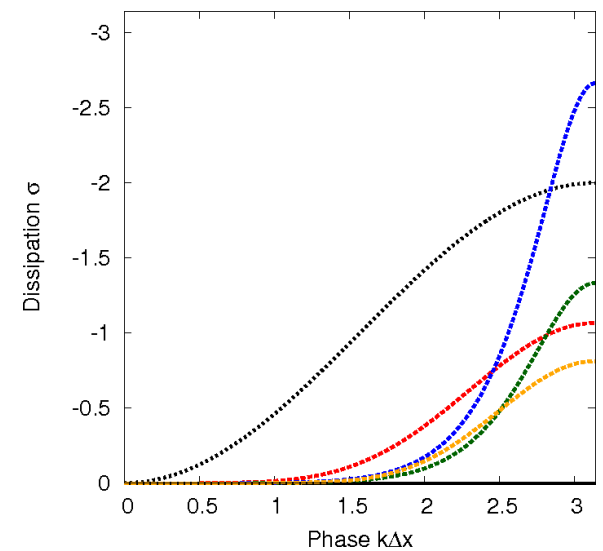
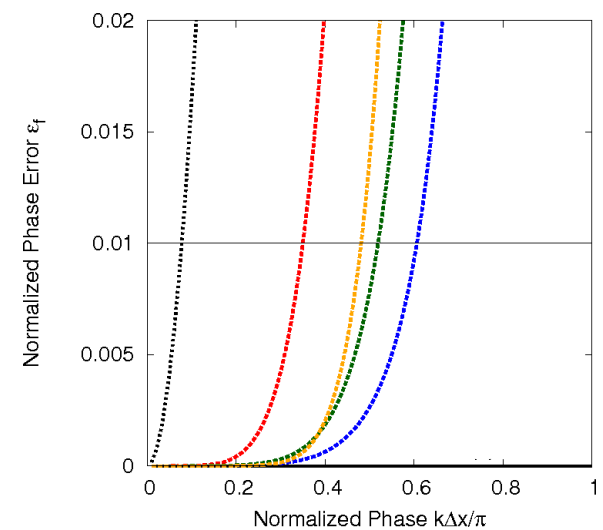
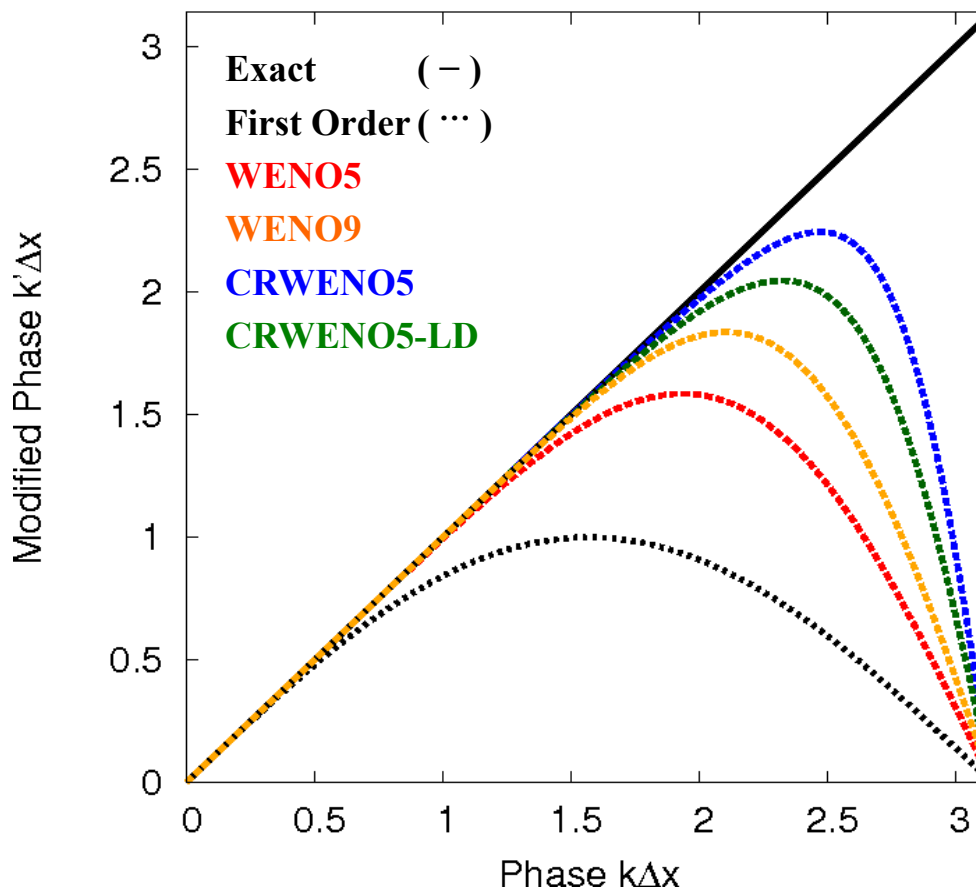
Taylor Series Analysis: **Dissipation** and **dispersion** errors

	<b>WENO5</b>	<b>CRWENO5</b>	<b>CRWENO5-LD</b>
<b>Dissipation</b>	$\frac{1}{60} \frac{\partial^6 f}{\partial x^6} \Big _j \Delta x^5$	$\frac{1}{600} \frac{\partial^6 f}{\partial x^6} \Big _j \Delta x^5$	$\frac{1}{1200} \frac{\partial^6 f}{\partial x^6} \Big _j \Delta x^5$
<b>Dispersion</b>	$\frac{1}{140} \frac{\partial^7 f}{\partial x^7} \Big _j \Delta x^6$	$\frac{1}{2100} \frac{\partial^7 f}{\partial x^7} \Big _j \Delta x^6$	$\frac{1}{2100} \frac{\partial^7 f}{\partial x^7} \Big _j \Delta x^6$

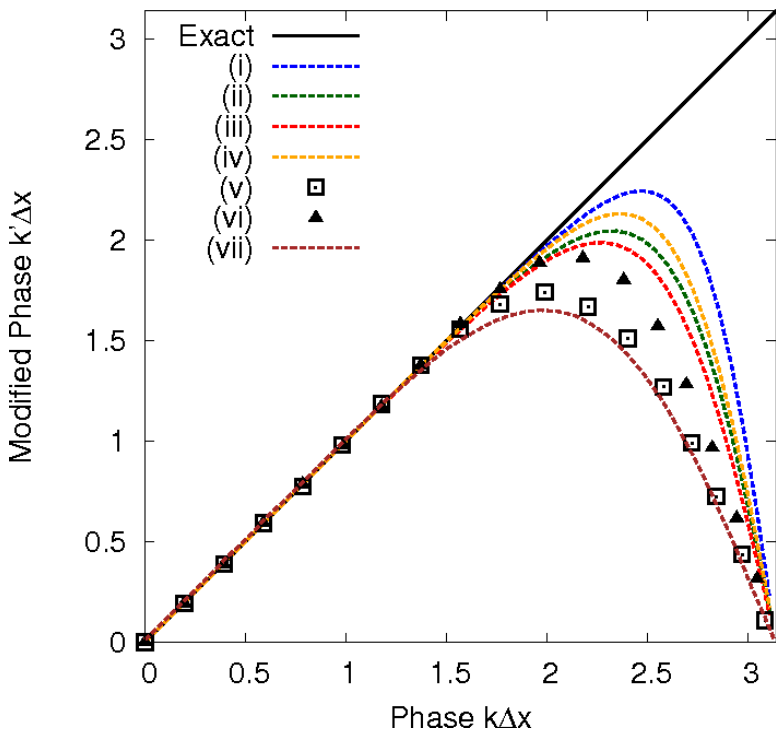


# Numerical Analysis

## Fourier Analysis: spectral properties



# Comparison of Spectral Resolutions



- i. CRWENO5
- ii. CRWENO5-LD
- iii. 6<sup>th</sup> order central compact (Lele, 1992)
- iv. 8<sup>th</sup> order central compact (Lele, 1992)
- v. WENO-SYMB0 ( $r=3$ ) (Martin, et. al., 2006)
- vi. WENO-SYMB0 ( $r=4$ ) (Martin, et. al., 2006)
- vii. WCNS5 (Deng & Zhang, 2000)

Comparison of **spectral resolution** and **bandwidth resolving efficiency** – CRWENO5 scheme with high-resolution schemes in literature

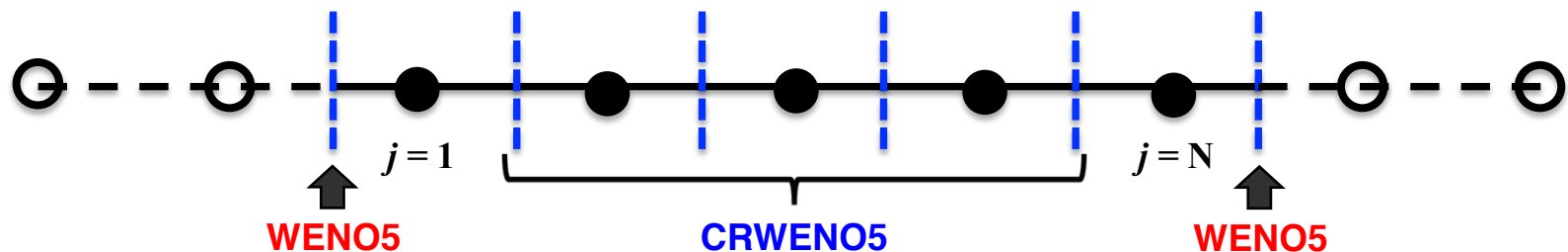
## Bandwidth Resolving Efficiency

WENO5 (Jiang & Shu, 1996)	0.35
WENO7 (Balsara & Shu, 2000)	0.42
WENO9 (Balsara & Shu, 2000)	0.48
<b>CRWENO5</b>	<b>0.61</b>
<b>CRWENO5-LD</b>	<b>0.52</b>
6th-order central compact (Lele, 1992)	0.50
8th-order central compact (Lele, 1992)	0.58
WENO-SYMB0 ( $r = 3$ ) (Martin, et. al., 2006)	0.49
WENO-SYMB0 ( $r = 4$ ) (Martin, et. al., 2006)	0.56

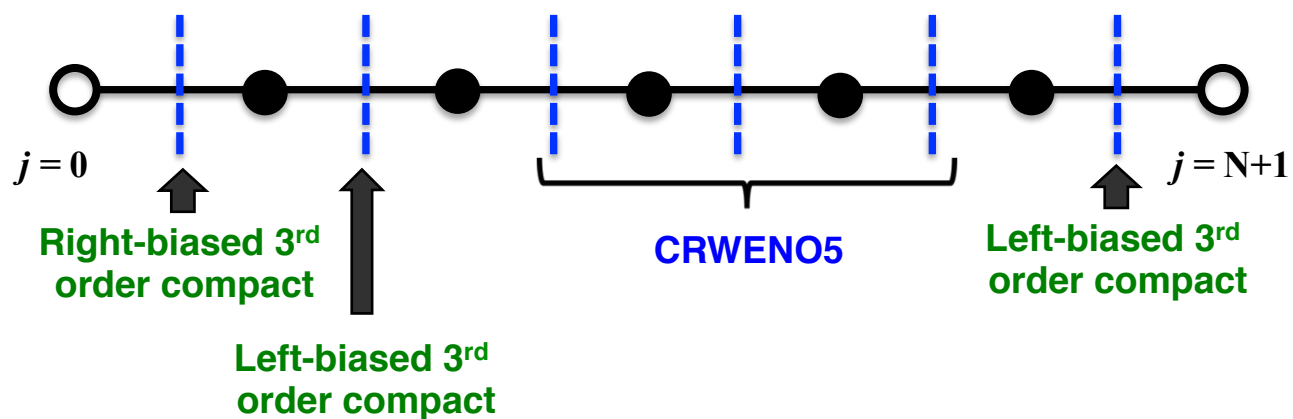


# Boundary Closure

Cell interface aligned with physical boundary – Boundary conditions implemented on “ghost cells”



Cell center coincident on physical boundary – Reduced-order / interior-biased interpolation scheme at interfaces near the boundary



# Scalar Conservation Laws

Schemes validated for the linear advection equation and the inviscid Burgers equation

## Smooth problems

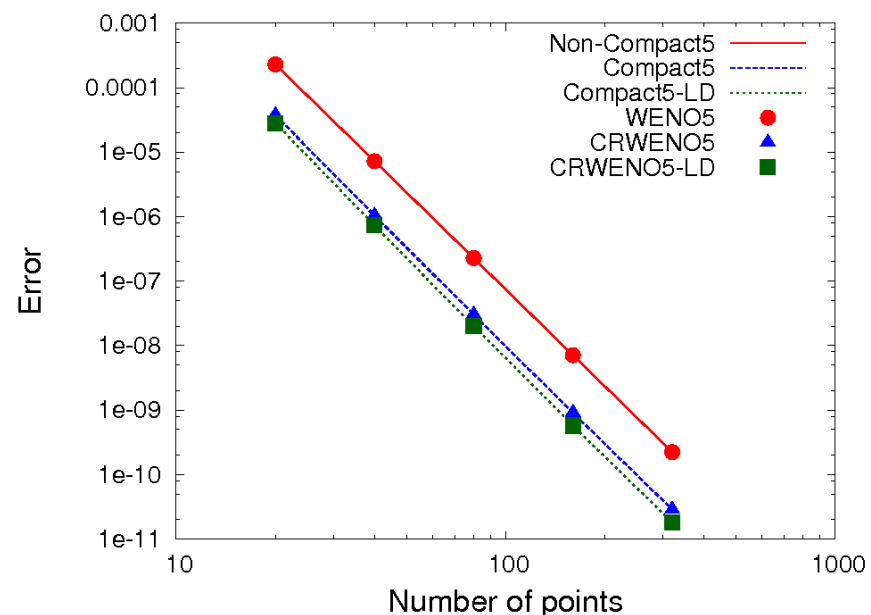
- 5<sup>th</sup> order convergence verified for the new schemes
- Errors for CRWENO5 order of magnitude lower than WENO5, errors for CRWENO5-LD half those of CRWENO5

## Linear advection equation

$$u_0(x) = \sin(2\pi x); 0 \leq x \leq 1$$

(Periodic domain)

Solution obtained after 1 cycle with TVD-RK3 time-stepping

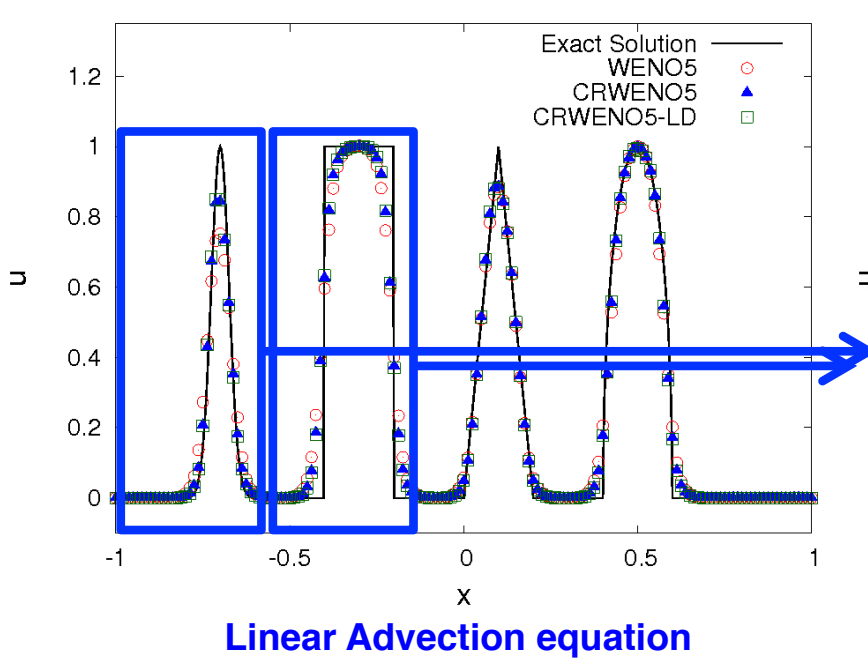


# Scalar Conservation Laws

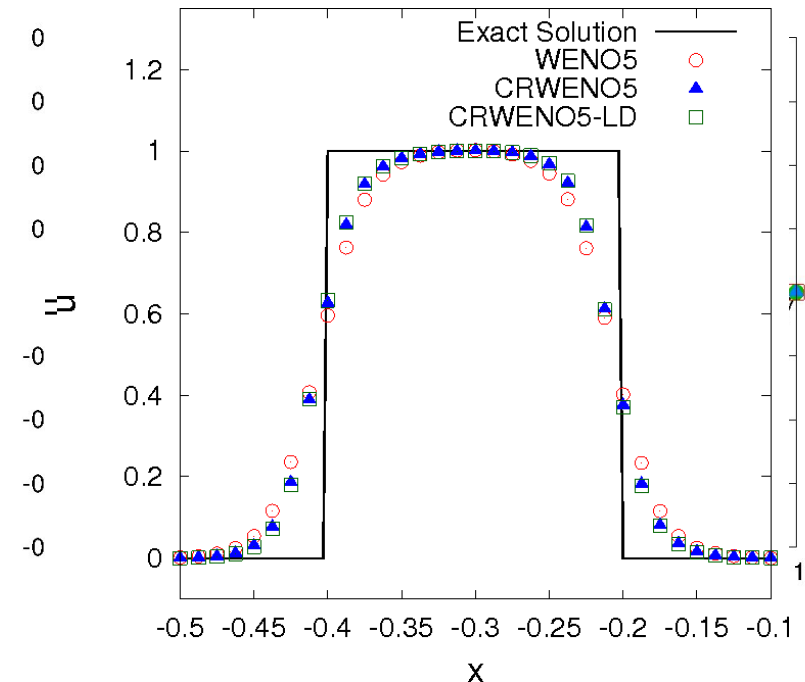
Schemes validated for the linear advection equation and the inviscid Burgers equation

## Discontinuous problems

- Non-oscillatory behavior validated across discontinuities
- CRWENO schemes show better resolution of discontinuous data (lower smearing and clipping)

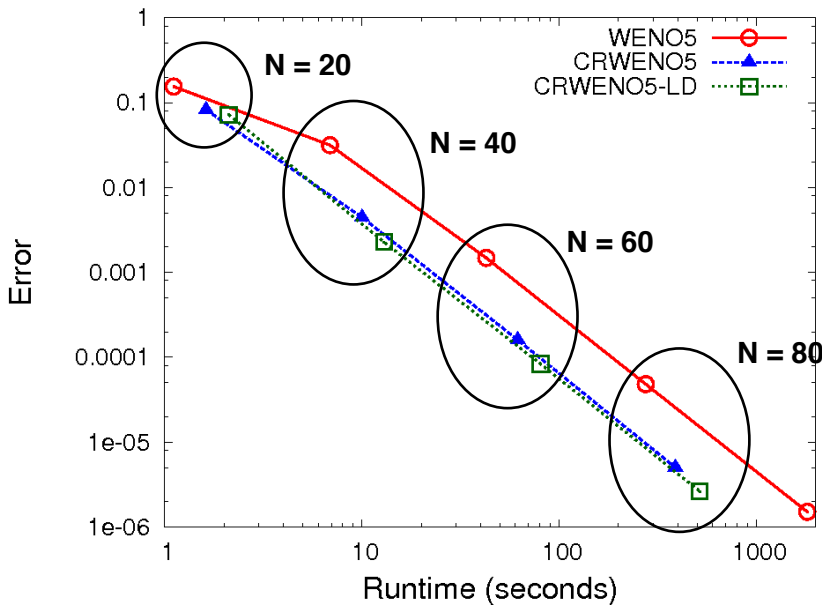


Linear Advection equation

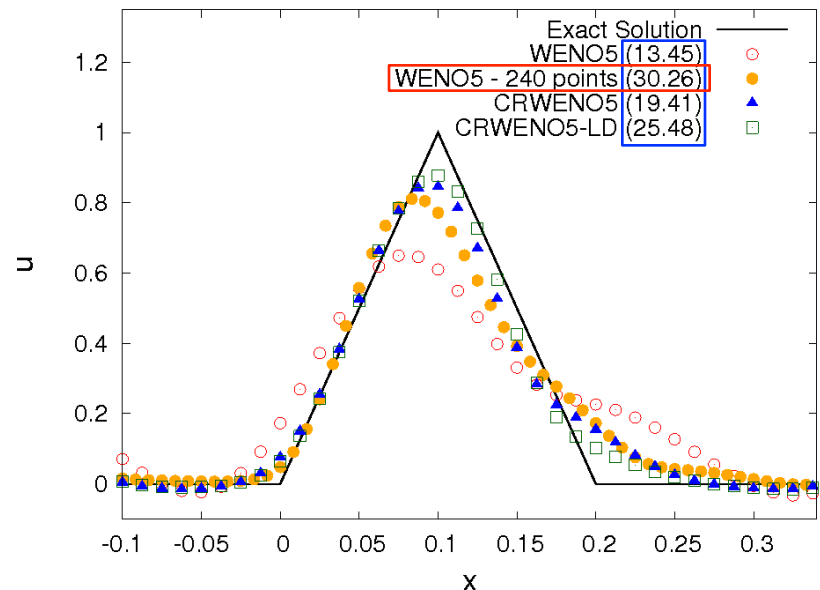


# Computational Efficiency

- CRWENO schemes require **solution to tridiagonal system** at each iteration (solution-dependent weights) → **Higher numerical cost** for same number of points
- Higher accuracy (error is  $1/10^{\text{th}}$  that of WENO) → Comparable solution obtained on coarser mesh → **Computationally more efficient**



Error vs. runtime for smooth problem



Periodic advection of a triangular wave after 100 cycles (120 point mesh)



# Implementation of Non-Linear Weights

- Definition of the WENO weights by Jiang & Shu (1996):

$$\alpha_k = \frac{c_k}{(\beta_k + \varepsilon)^p} \quad p = 2 \quad \varepsilon = 10^{-6}$$

CRWENO5-JS

- $\varepsilon$  – sensitivity: Lower values of  $\varepsilon$  ( $10^{-40}$ ) results in sub-optimal convergence for smooth problems with critical points (vanishing derivatives)
- Excessive dissipation: Original weights defined by Jiang & Shu were found to be too dissipative across discontinuities

- Alternative formulations proposed in literature:

- Mapped WENO (Henrick, Aslam & Powers, 2005): Defined a mapping function that improved convergence to WENO weights

$$g_k(\omega) = \frac{\omega(c_k + c_k^2 - 3c_k\omega + \omega^2)}{c_k^2 + \omega(1 - 2c_k)}$$

CRWENO5-M

- WENO-Z (Borges, et. al., 2008)

- ESWENO (Yamaleev & Carpenter, 2009)

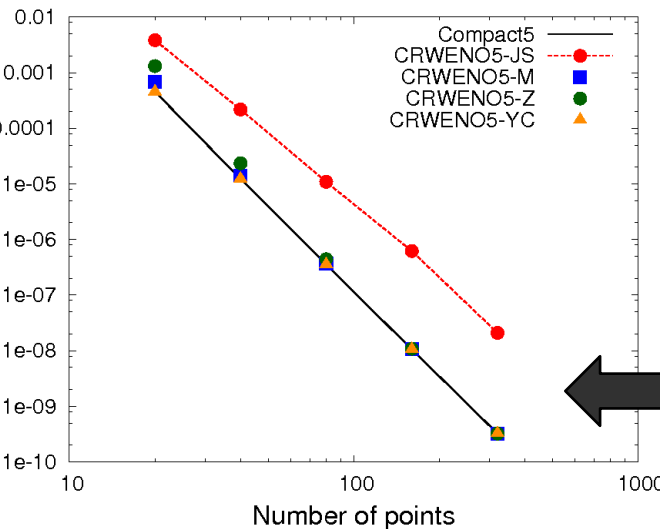
$$\alpha_k = c_k \left[ 1 + \left( \frac{\tau}{\varepsilon + \beta_k} \right)^p \right]$$

CRWENO5-Z

CRWENO5-YC

- These improved convergence and resolution of the WENO schemes

# Implementation of Non-Linear Weights



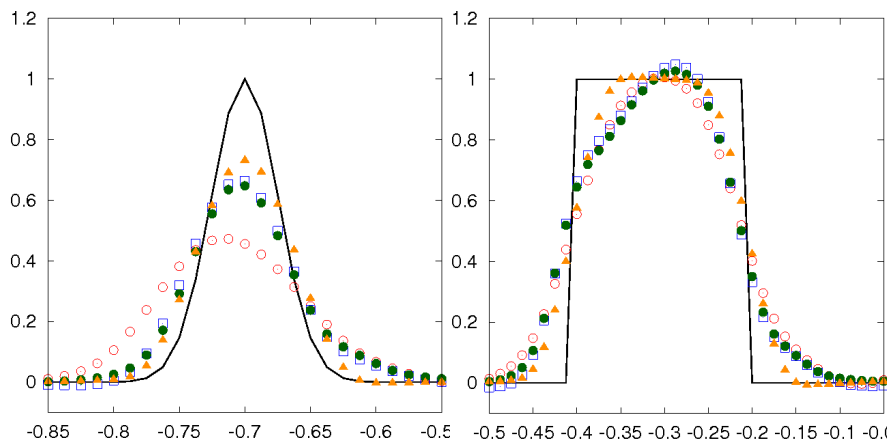
- Improved accuracy and convergence for smooth problems
- Sharper resolution for extrema and discontinuities
- Yamaleev & Carpenter weights show non-oscillatory behavior for higher derivatives (for this case)

**Solution after 1 cycle**

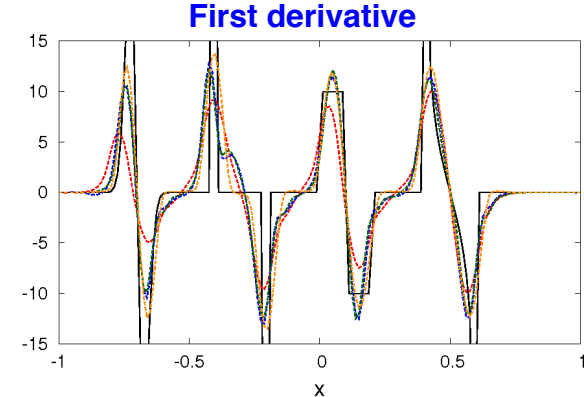
$$u_0(x) = \sin\left(\pi x - \frac{\sin(\pi x)}{\pi}\right)$$

$-1 \leq x \leq 1$  (Periodic)

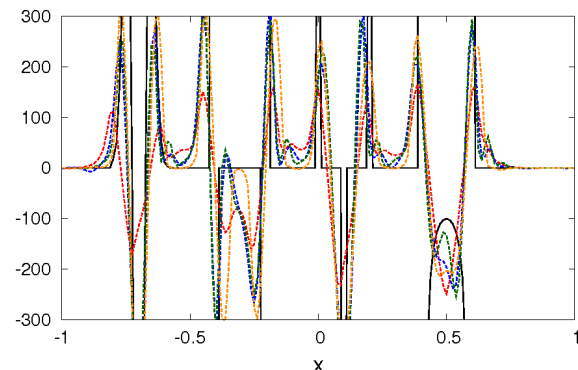
**Solutions of exponential and square waves after 50 cycles**



**CRWENO5-JS**  
**CRWENO5-M**  
**CRWENO5-Z**  
**CRWENO5-YC**



**Second derivative**





# Application to Inviscid Euler Equations



# Euler Equations

- Compressible Euler equations in 1D given by

$$\frac{\partial}{\partial t} \begin{bmatrix} \rho \\ \rho u \\ e \end{bmatrix} + \frac{\partial}{\partial x} \begin{bmatrix} \rho u \\ \rho u^2 + p \\ (e + p)u \end{bmatrix} = 0$$

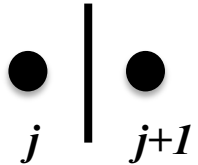
$\rho$  = Density  
 $u$  = Velocity  
 $p$  = Pressure  
 $e = \frac{p}{\gamma - 1} + \frac{1}{2} \rho u^2$  (Internal energy)

- In the form of a general hyperbolic PDE  $u_t + f(u)_x = 0$
- Extension of scalar interpolation schemes to a system of equations
  - Component-wise reconstruction of **conserved variables** ( $\rho, \rho u, e$ )
  - Reconstruction of **primitive (flow) variables** ( $\rho, u, p$ )
  - Reconstruction of **characteristic variables**
- Extension to conserved/primitive variables trivial
  - Solution of **D+2 tridiagonal systems** of equations (D is the number of dimensions)



# CRWENO for Euler Equations

Characteristic based reconstruction respects the physics of the problem – 1D scalar wave propagation along each characteristic



$$a\alpha_{j-1/2}^k + b\alpha_{j+1/2}^k + c\alpha_{j+3/2}^k = \tilde{a}\alpha_{j-1}^k + \tilde{b}\alpha_j^k + \tilde{c}\alpha_{j+1}^k \quad (\alpha_i^k = \mathbf{l}_{j+1/2}^k \cdot \mathbf{f}_i)$$



$\mathbf{U}^{\text{avg}}$  (Roe averaged)

$$\hookrightarrow \lambda_{j+1/2}^k, \mathbf{l}_{j+1/2}^k, \mathbf{r}_{j+1/2}^k$$

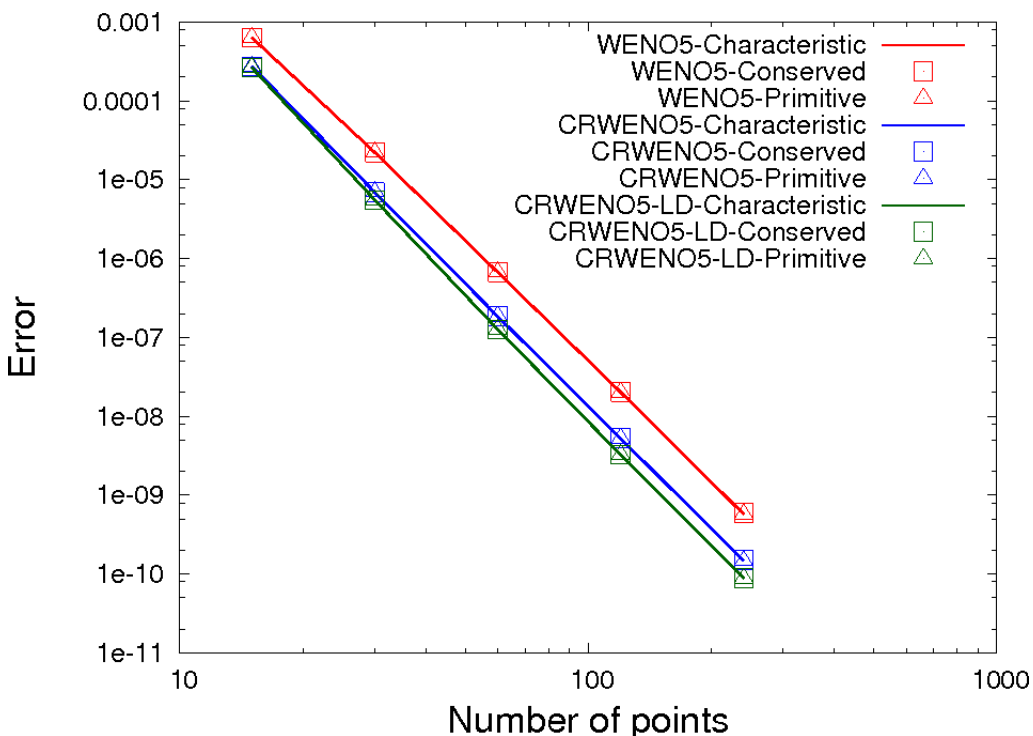
Eigenvalues, left and right eigenvectors

$$\begin{aligned} & a(l_{j+1/2}^{k1} f_{j-1/2}^1 + l_{j+1/2}^{k2} f_{j-1/2}^2 + l_{j+1/2}^{k3} f_{j-1/2}^3) \\ & + b(l_{j+1/2}^{k1} f_{j+1/2}^1 + l_{j+1/2}^{k2} f_{j+1/2}^2 + l_{j+1/2}^{k3} f_{j+1/2}^3) = \tilde{a}\alpha_{j-1}^k + \tilde{b}\alpha_j^k + \tilde{c}\alpha_{j+1}^k \\ & + c(l_{j+1/2}^{k1} f_{j+3/2}^1 + l_{j+1/2}^{k2} f_{j+3/2}^2 + l_{j+1/2}^{k3} f_{j+3/2}^3) \end{aligned}$$

- Results in a block tri-diagonal linear system along each dimension (as compared to tri-diagonal system for conserved/primitive reconstruction)
- For multi-dimensions, solution of linear system required along each grid line
- Upwinding –
  - Left and right biased fluxes computed
  - Roe-Fixed formulation used

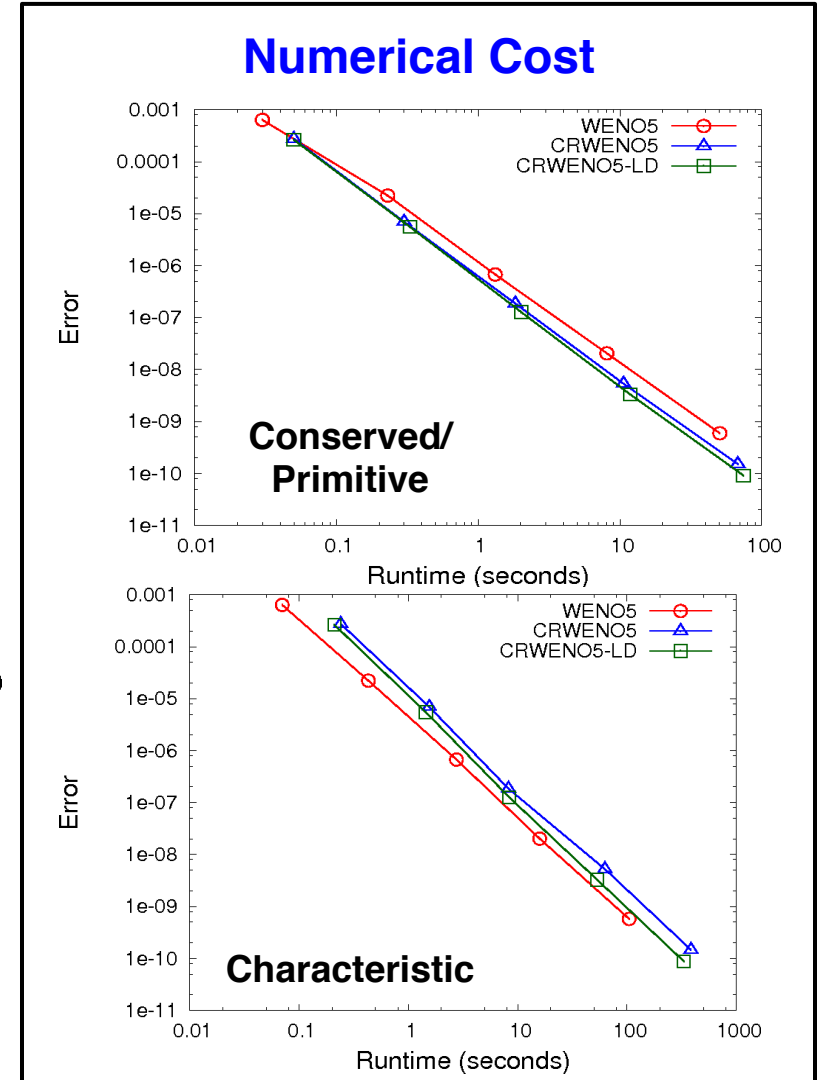
$$\alpha_{j+1/2}^{k,L}, \alpha_{j+1/2}^{k,R} \Rightarrow \alpha_{j+1/2}^k$$

# Entropy Wave Advection

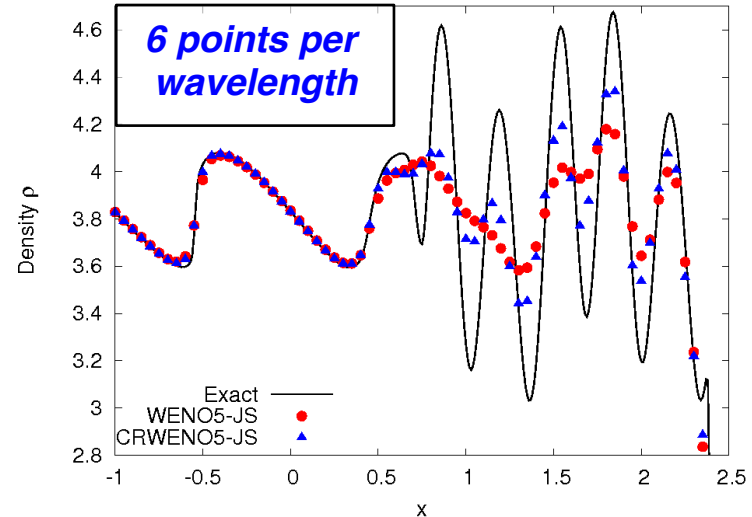
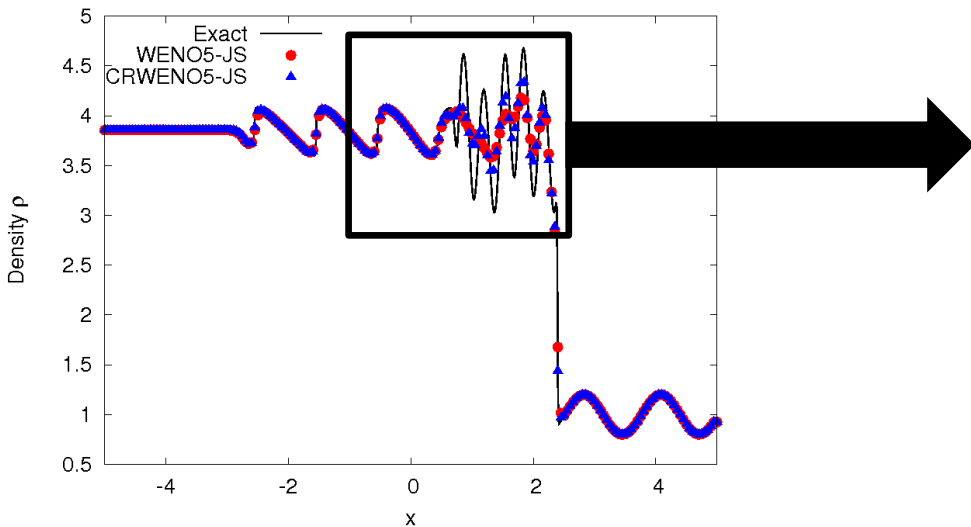


## Reconstruction of characteristic, primitive & conserved variables

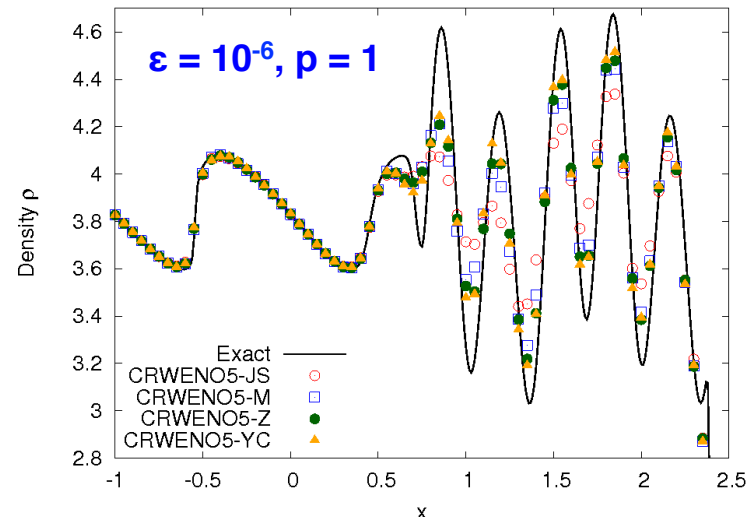
- Accuracy** – CRWENO5 errors  $1/10^{\text{th}}$  that of WENO5
- Smooth problem** – Reconstruction of conserved, primitive and characteristic yield identical solutions
- Computational expense** - CRWENO5 is more efficient for conserved/primitive reconstruction, but not for characteristic reconstruction



# Shock – Entropy Interaction

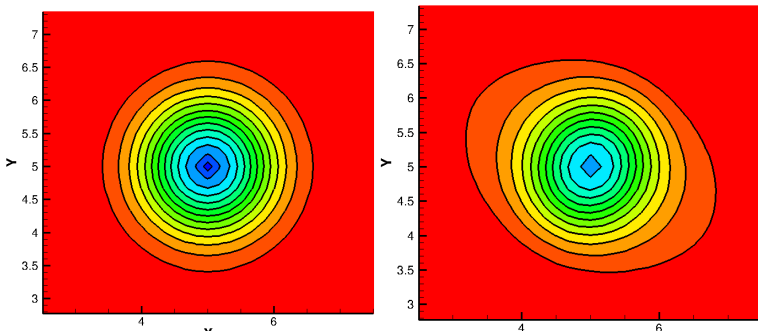


- Interaction of a shock wave with a density wave resulting in **high-frequency waves** and **discontinuities**
- CRWENO scheme shows **better resolution of high-resolution waves** than WENO5
- Further improvement by using the **alternative formulations** for the WENO weights

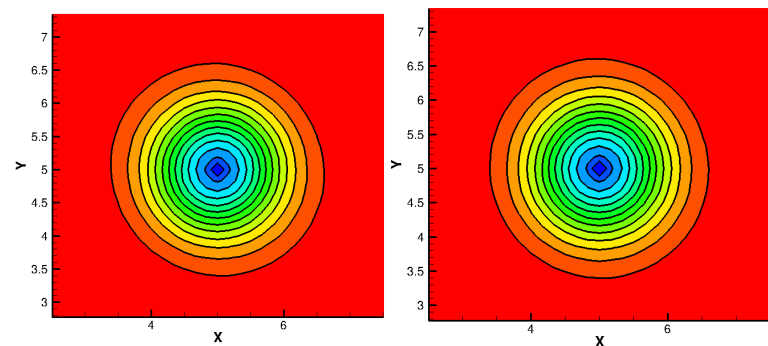


# Isentropic Vortex Convection

**Solution after travelling 1000 core radii**  
**Compact schemes show better shape and strength preservation for long term convection**

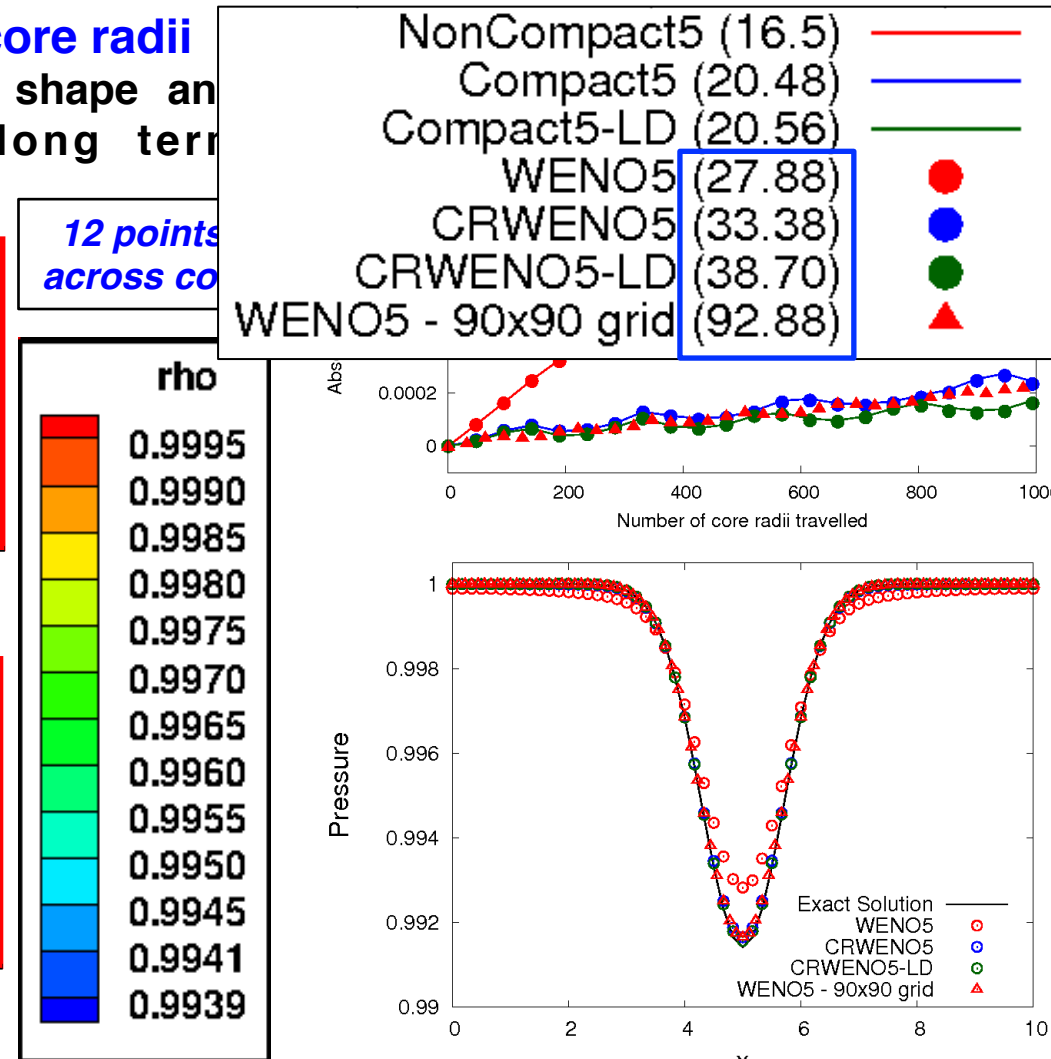


Initial



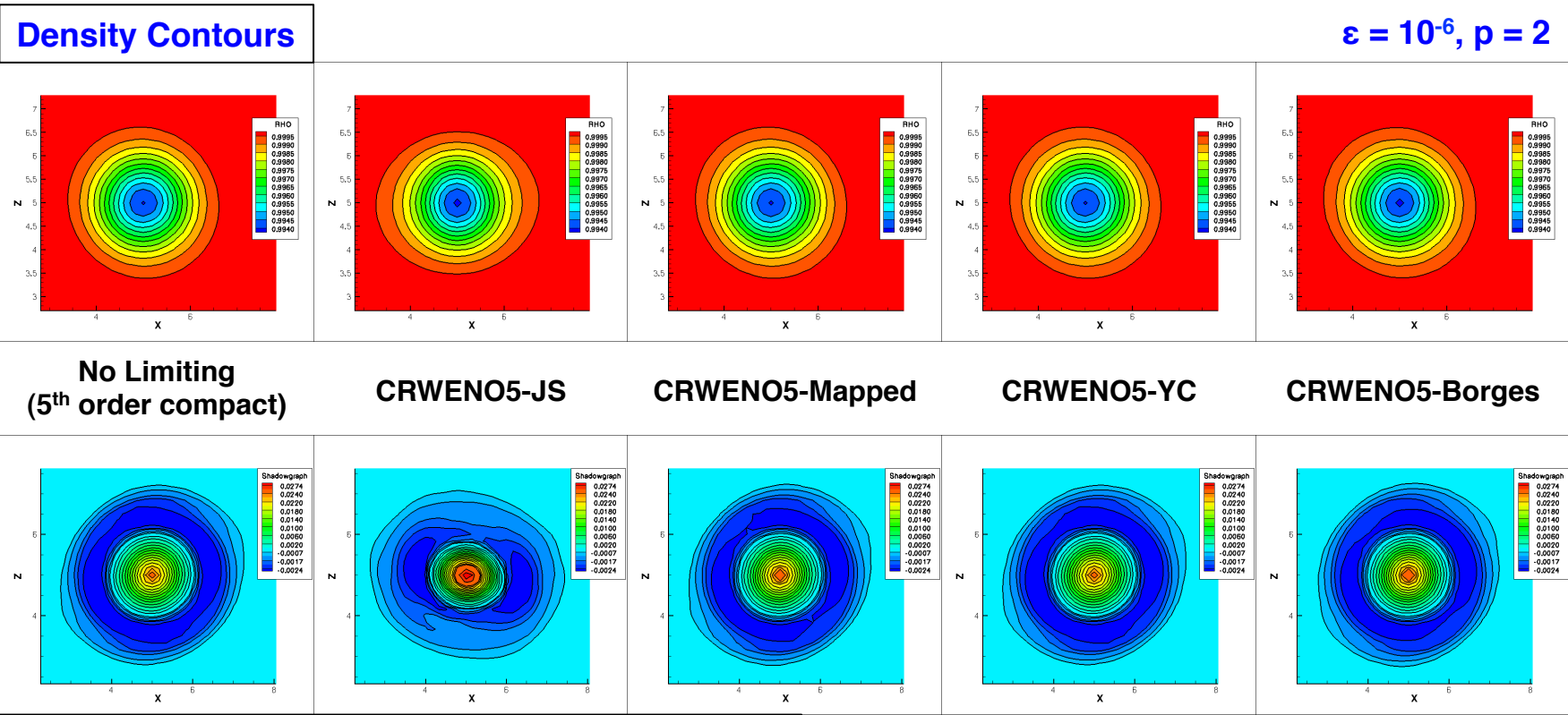
CRWENO5

CRWENO5-LD



# ISENTROPIC VORTEX CONVECTION

Long term inviscid convection (1000 core radii) – Preservation of strength and shape

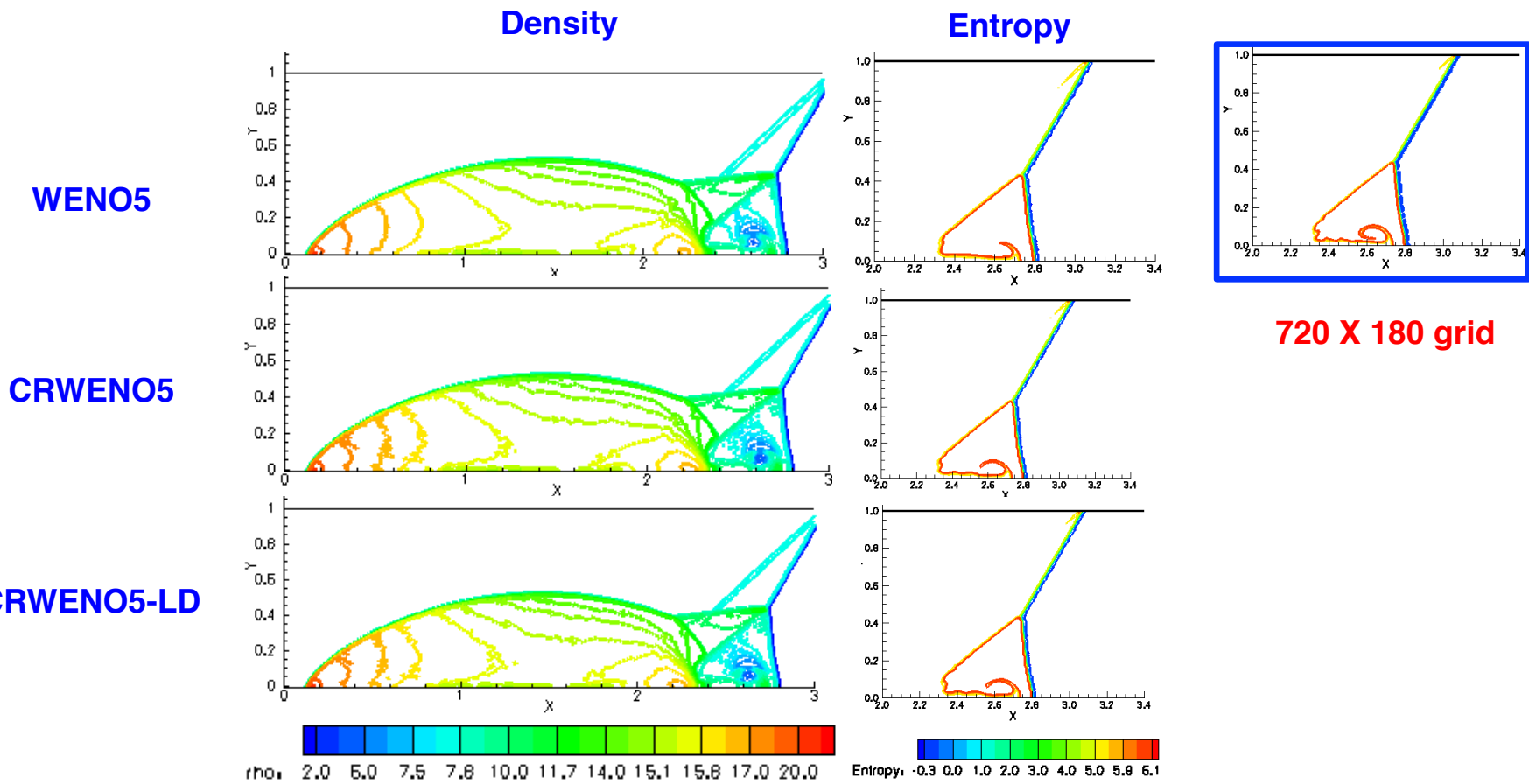


- Smooth, non-oscillatory density field for all schemes (almost identical)
- Oscillations in 2<sup>nd</sup> derivative for CRWENO5-JS & CRWENO5-Mapped, while CRWENO5-YC and CRWENO5-Borges are smooth

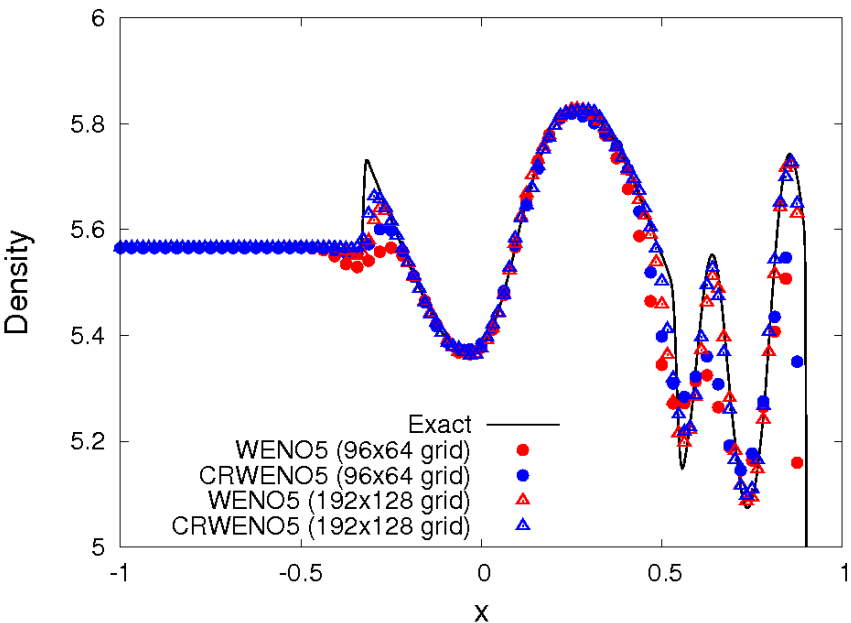
# Double Mach Reflection

Double Mach Reflection of a Mach 10 shock on a 480 X 120 grid

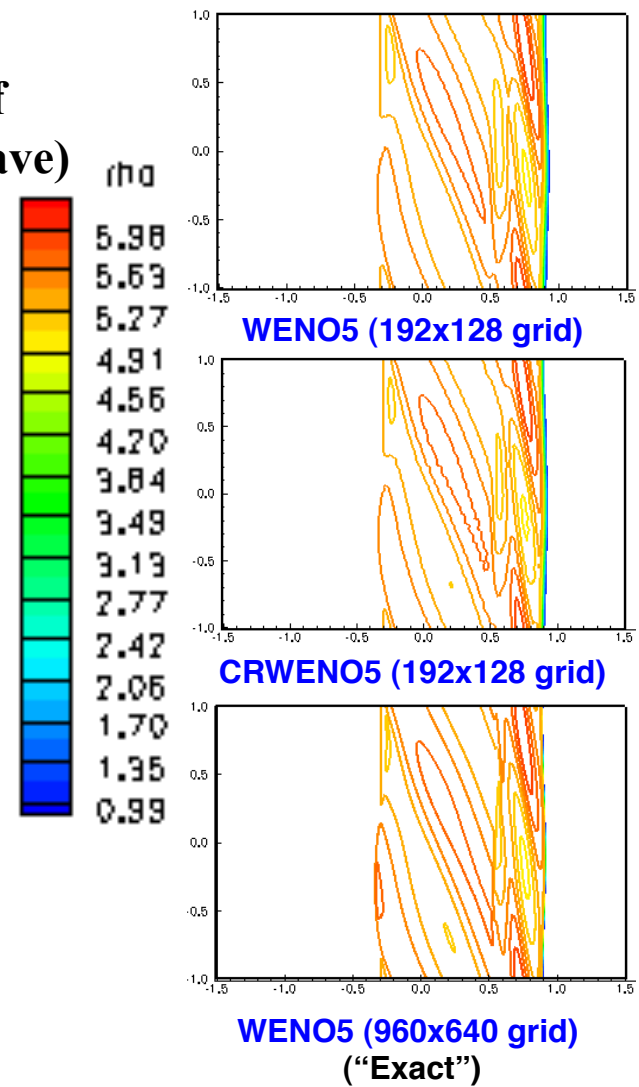
- CRWENO schemes validation for 2D problem with strong discontinuities
- Better capturing of the contact discontinuity roll-up



# Shock – Vorticity Interaction



$\theta = \pi/6$   
(Angle of  
vorticity wave)



## Interaction of a shock with a vorticity wave:

- Accurate capturing of acoustic, vorticity and entropy waves
- Solutions obtained on 96x64 and 192x128 grids
- CRWENO5 shows reduced clipping of the waves at both grid resolutions



# Integration with a Finite-Volume Navier-Stokes Solver



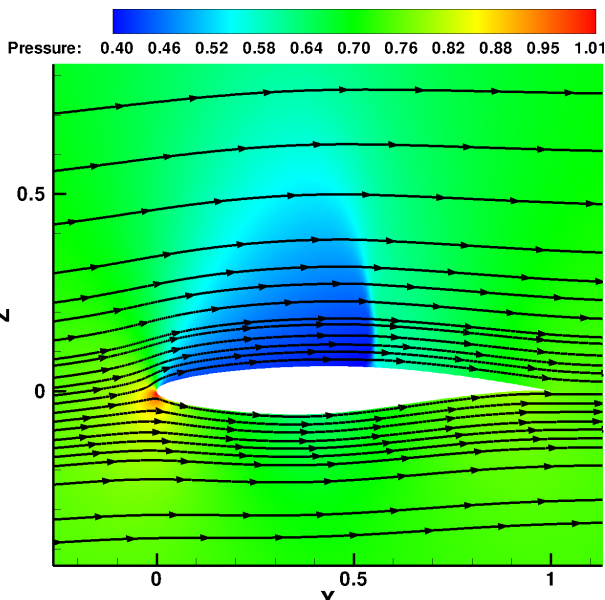
# Baseline Solver

Integration of the CRWENO scheme with a compressible Navier Stokes solver for overset structured meshes

- **Time Marching:** 2<sup>nd</sup> order Backward Differencing (BDF2) and 3<sup>rd</sup> order Total Variation Diminishing Runge Kutta (TVDRK3)
- **Dual time-stepping** for time-accurate computations
- **Implicit Inversion:** Diagonalized ADI and LU-SGS
- **Spatial reconstruction:**
  - 5<sup>th</sup> order CRWENO scheme (**compact**)
  - 3<sup>rd</sup> order MUSCL and 5<sup>th</sup> order WENO schemes (**non-compact**)
- **Upwinding:** Roe's flux differencing
- **Turbulence Modeling:** Spallart-Almaras one-equation model
- **Implicit hole-cutting** for overset meshes
- **Viscous Terms** discretized by 2<sup>nd</sup> order central differences



# Steady Flow around RAE2822 Airfoil

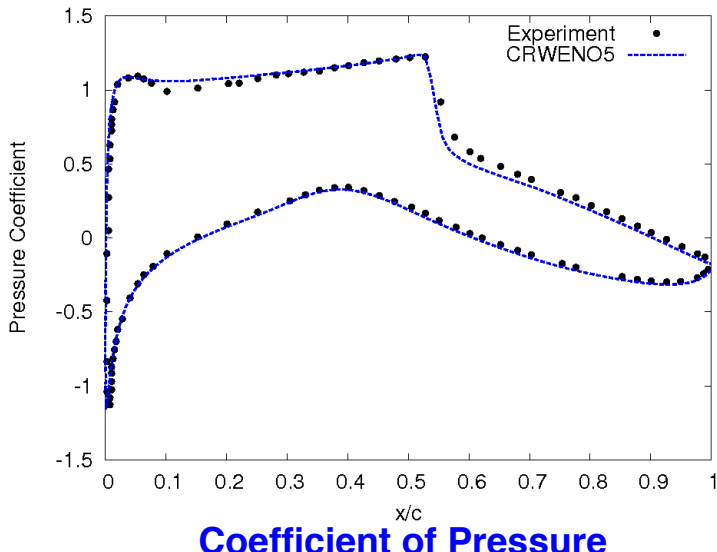


Turbulent, transonic flow around RAE2822

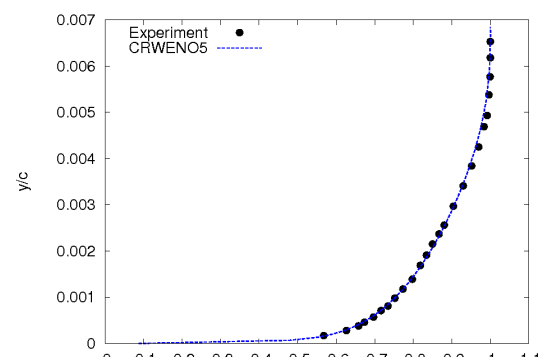
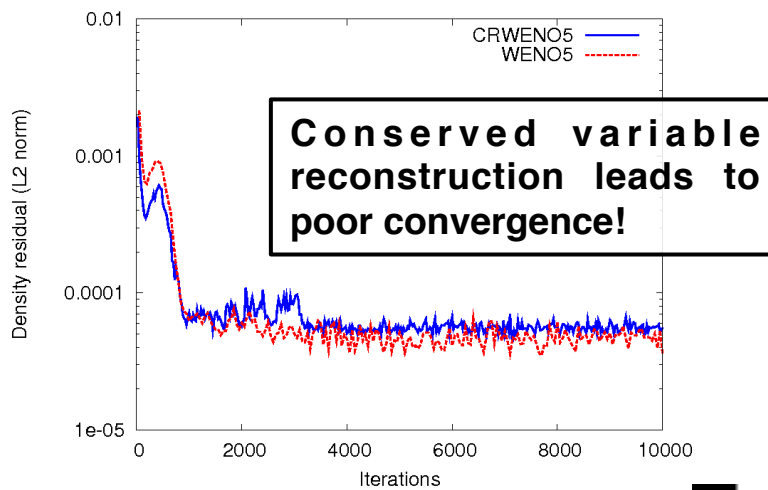
Flow Conditions:  
Reynolds number 6.5 million, angle of attack  $2.51^\circ$ , freestream Mach number 0.731

Numerical Solution:  
Grid: 521x171 C-type  
Outer boundary: 50c  
CRWENO5 in space  
BDF2 in time

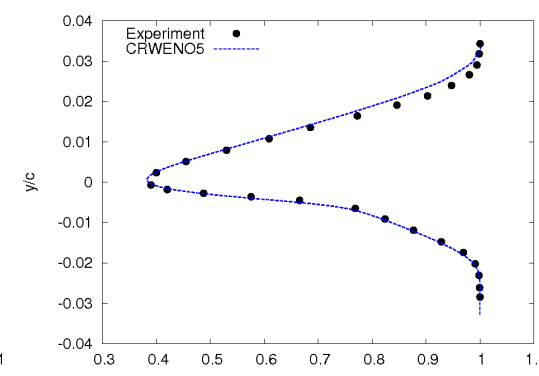
Validation w/ expt. results



Coefficient of Pressure



Boundary Layer and Wake velocity profiles

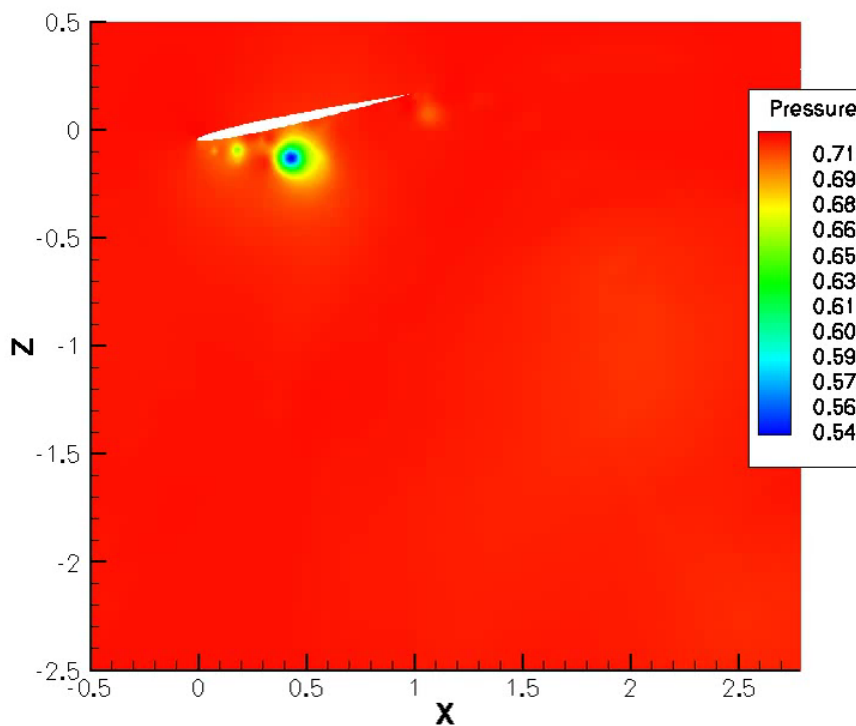




# Pitching – Plunging NACA0005

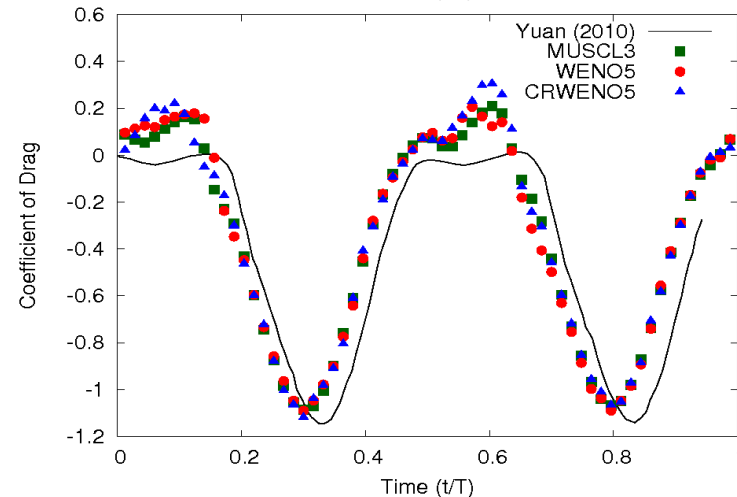
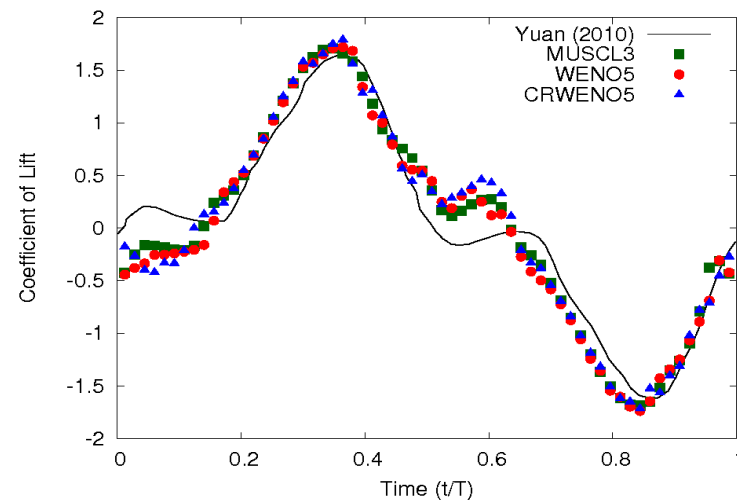
## Flow Conditions

Reynolds No. = 15000, Freestream Mach = 0.1  
Pitch amplitude = 40°, Plunge amplitude = 1.0  
Reduced frequency = 0.795



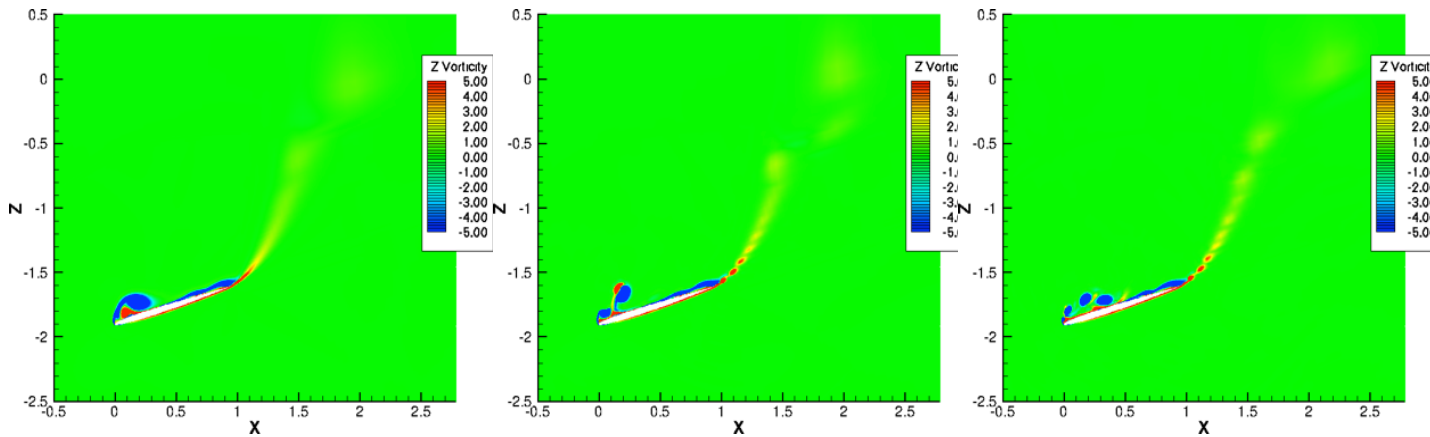
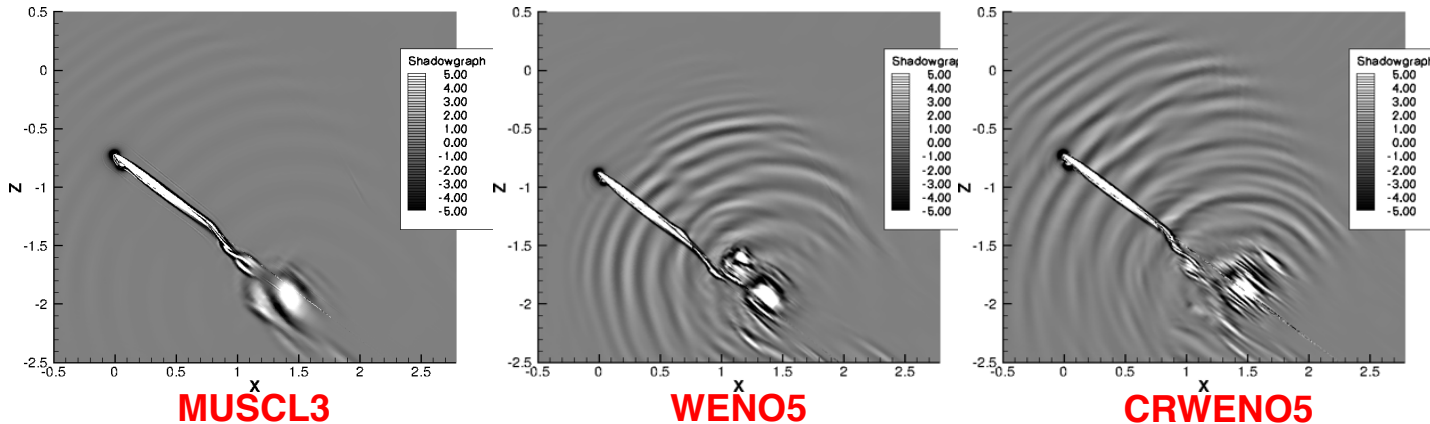
Grid dimensions: 391x161

Time stepping: BDF2 w/ 15 sub-iterations



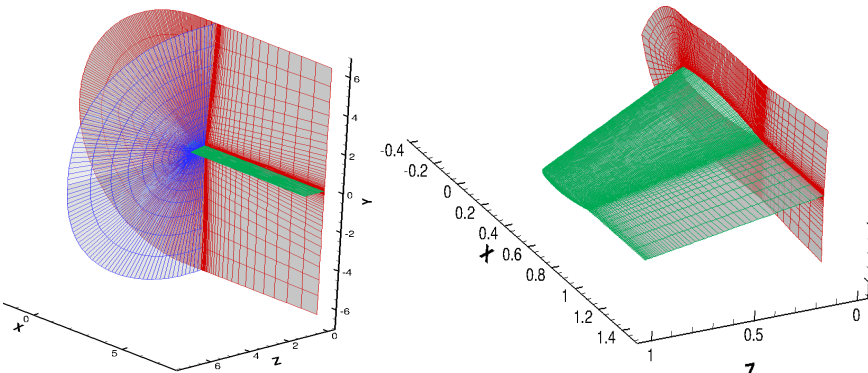
Lift and drag over one cycle

# Pitching – Plunging NACA0005



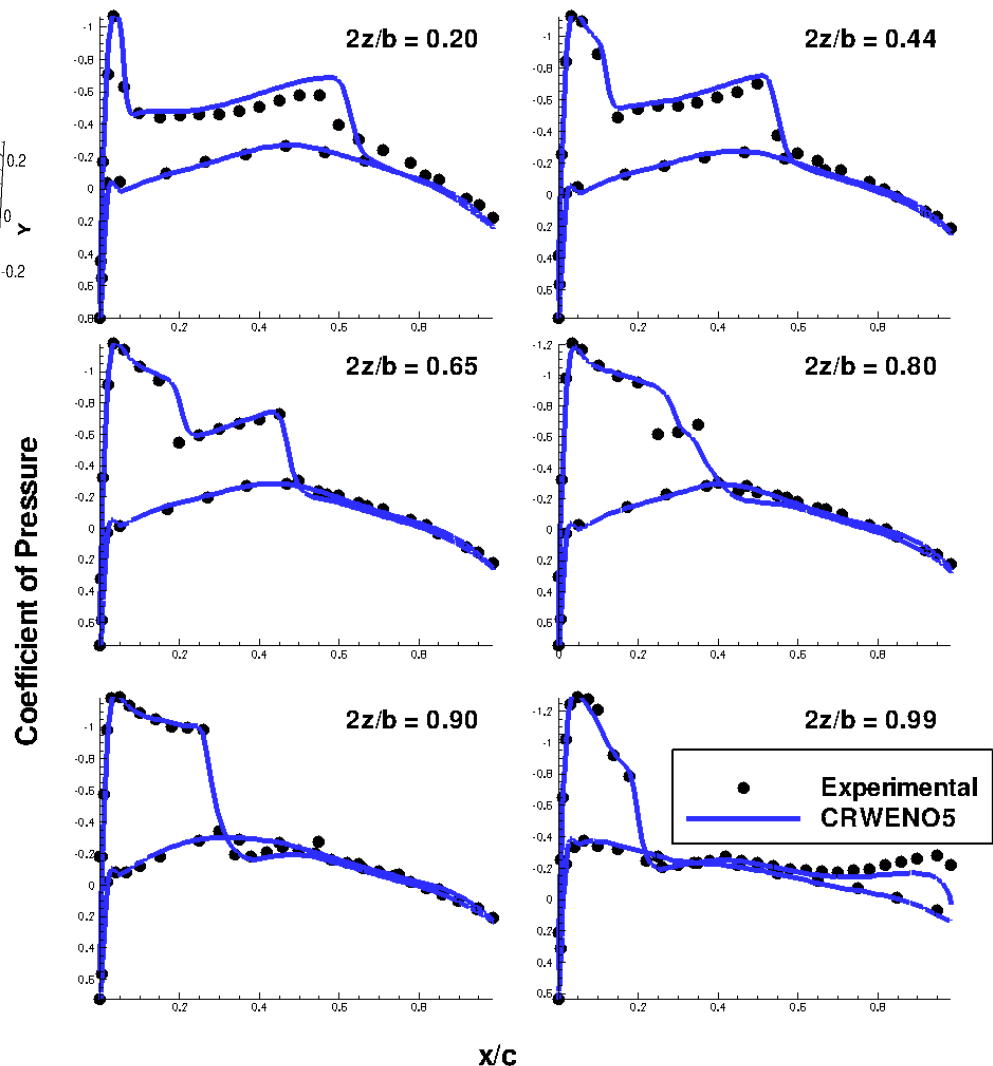
CRWENO5 shows improvement in capturing acoustic waves and vortical structures

# ONERA-M6 Wing

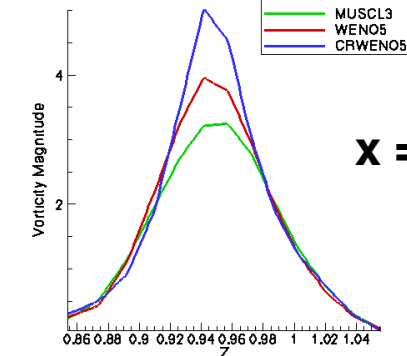
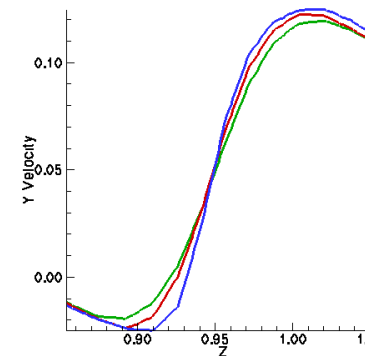
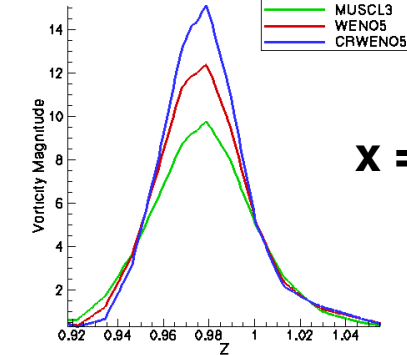
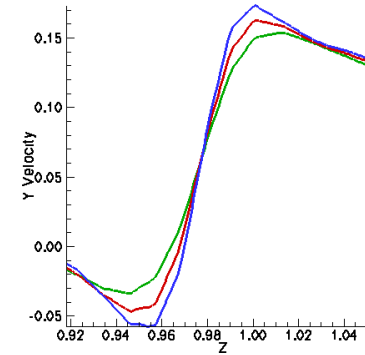
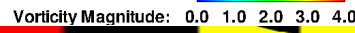
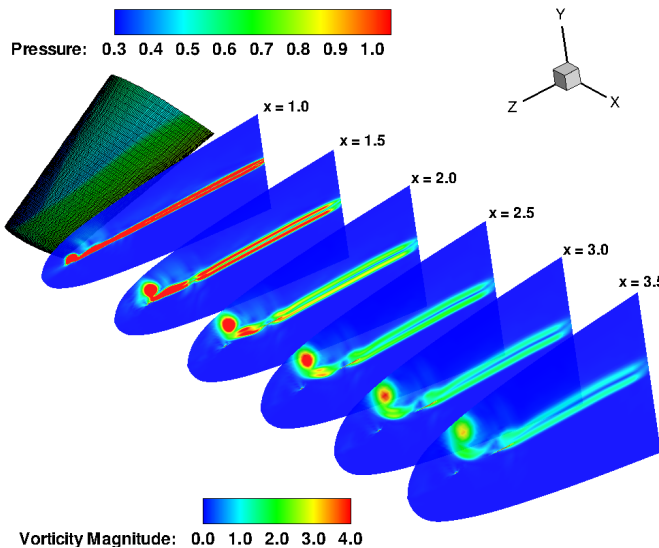
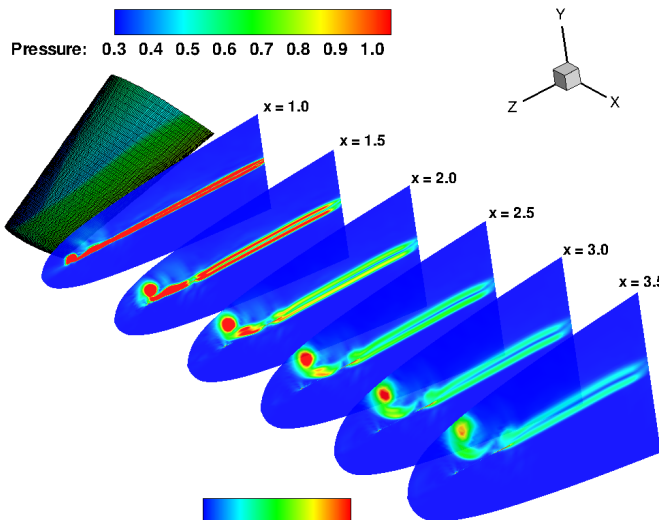
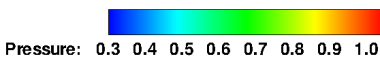


ONERA-M6 grid

- Steady, transonic flow around the ONERA-M6 wing
- C-O mesh with **289x65x49** points
- Freestream Re = **21.67 million**
- Freestream Mach number = **0.84**
- Angle of attack = **3.06°**
- Surface pressure coefficient validated with experimental data



# ONERA-M6 Wing



**CRWENO5 shows an improvement in the tip vortex resolution and preservation in the wake region**

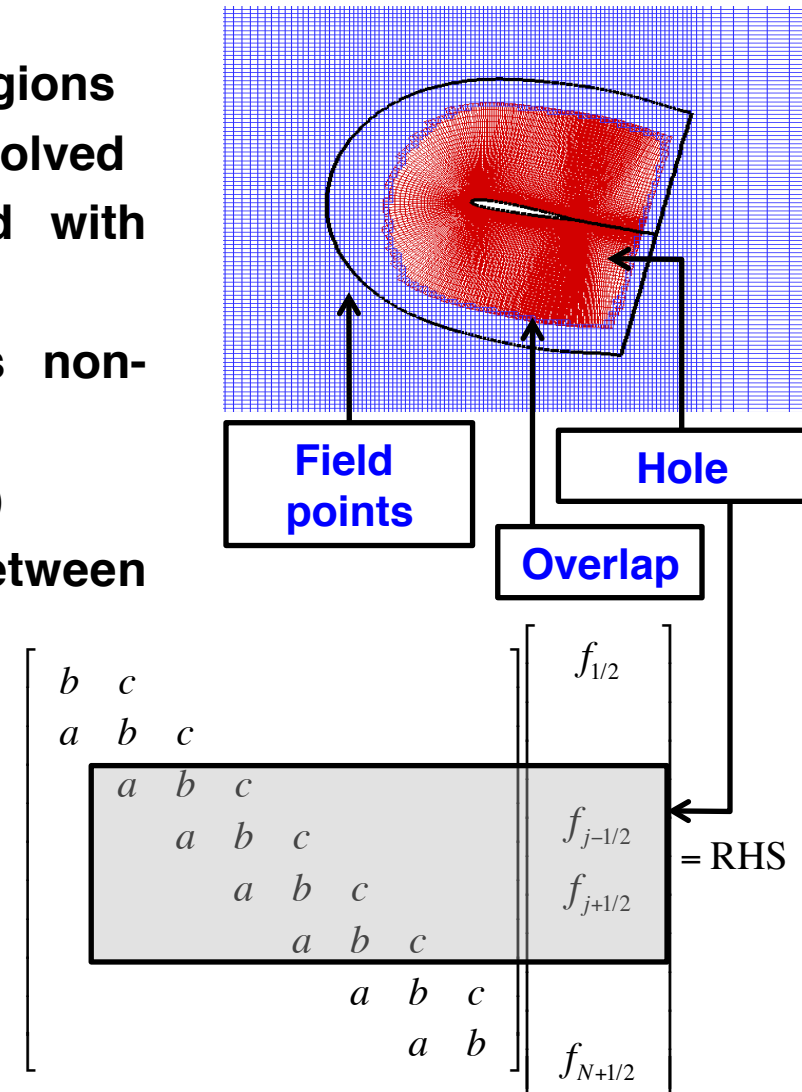
# Overset Grids

## Solution algorithm on overset meshes

- Identification of **field**, **overlap** and **hole** regions
- Field points → Governing equations are solved
- Overlap region → Solution exchanged with other meshes
- Hole region → Blanked out, contains non-physical values
- Implicit Hole-Cutting (Lee & Baeder, 2008)
- Tri-linear interpolation of solution between donor and receiver points

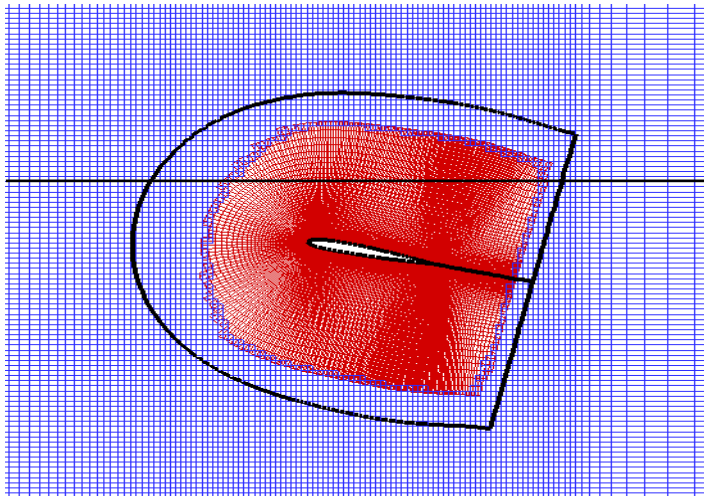
## Application of **compact** schemes

- Coupled solution for the interface fluxes
- Solution in **hole region coupled** with solution at field points
- System of equations contain non-physical values from the hole region



# CRWENO on Overset Grids

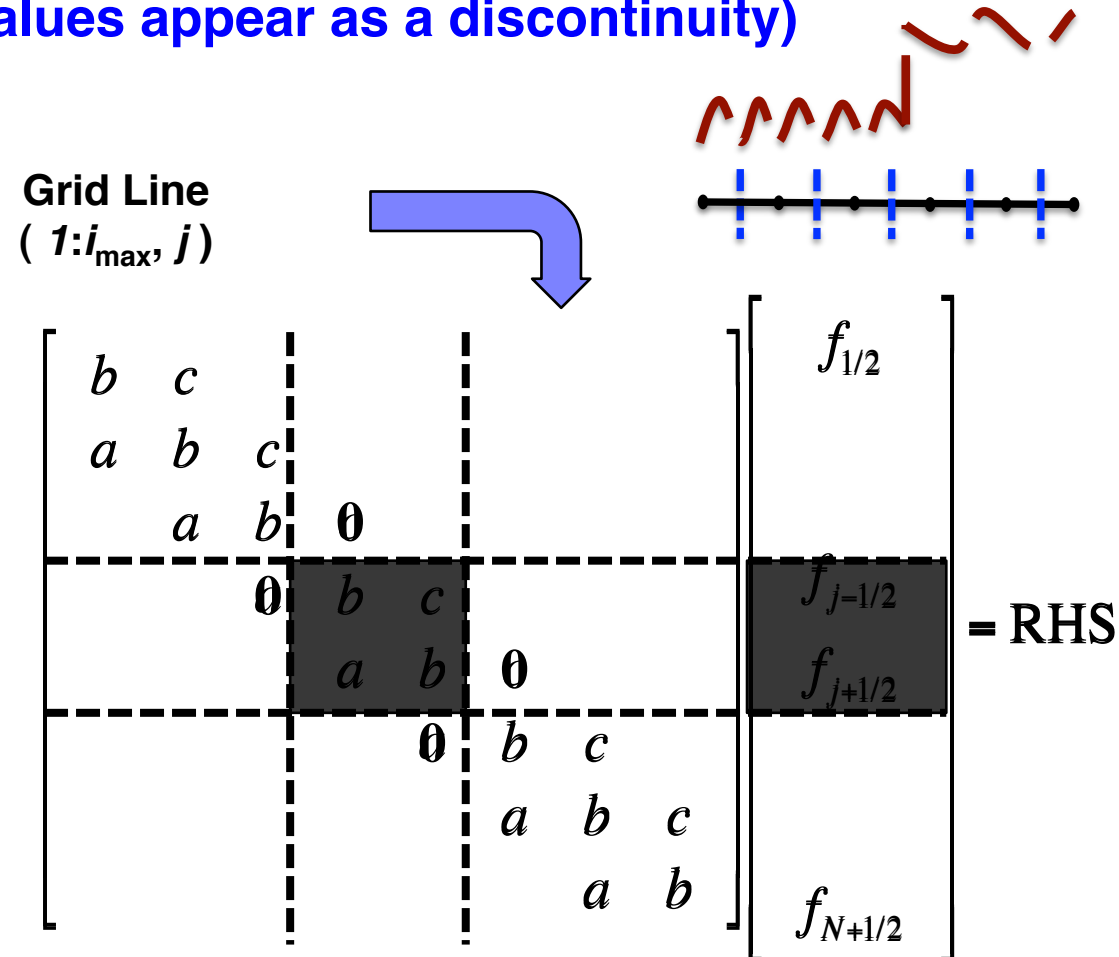
Behavior across discontinuity  $\leftrightarrow$  Behavior across hole cut  
 (Non-physical values appear as a discontinuity)



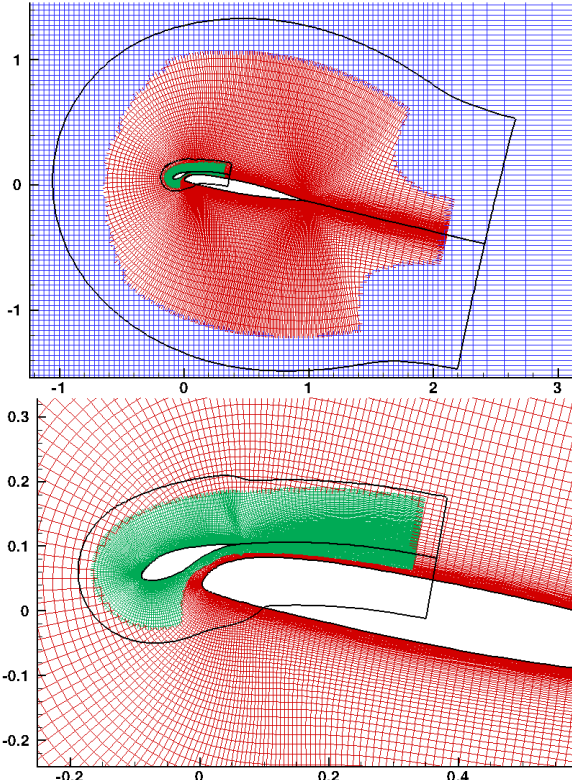
Adaptive stenciling of  
 the CRWENO scheme



Decoupling of solution  
 between field and hole  
 points



# SC2110 Airfoil w/ Slat in Wind Tunnel

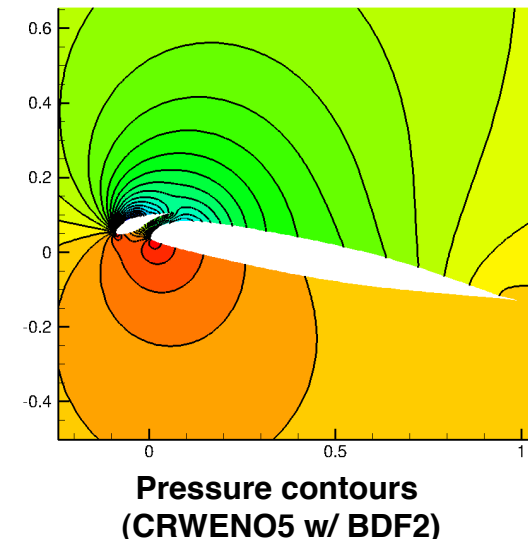


**Wind Tunnel Mesh –**  
Clustered Cartesian,  
151x101 points

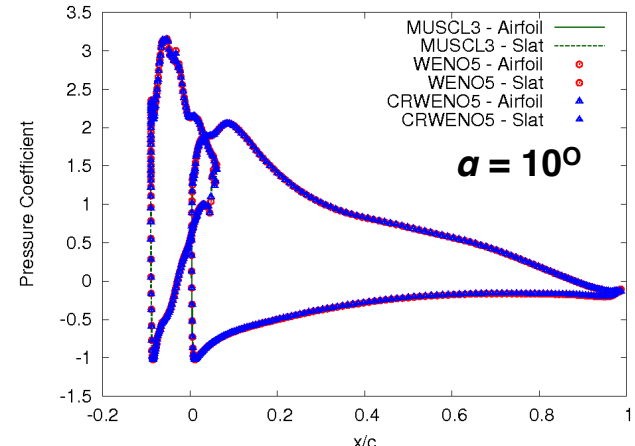
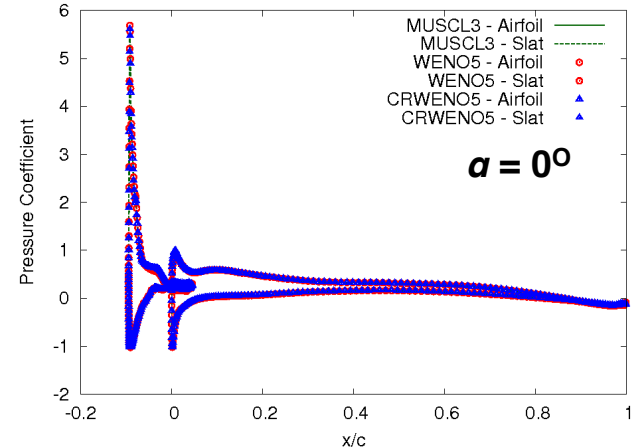
**Airfoil Mesh – C-type,**  
365x138 points

**Slat Mesh – C-type,**  
317x97 points

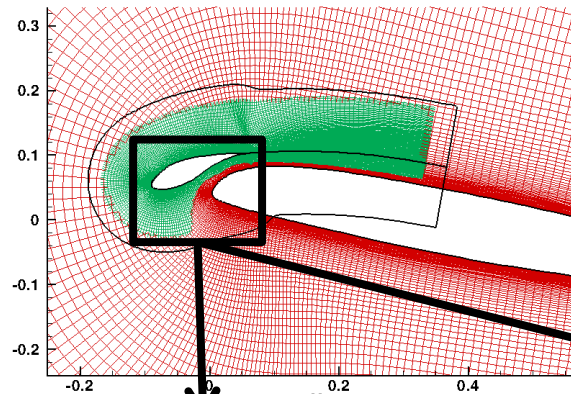
**Flow Conditions:**  
Reynolds number = 4.15e6  
Freestream Mach = 0.283  
Angle of Attack = 0°, 10°



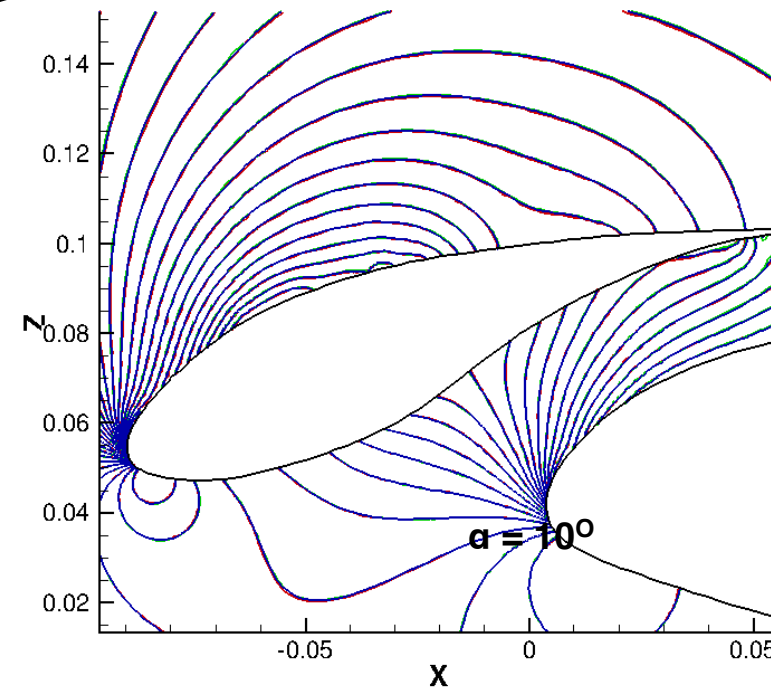
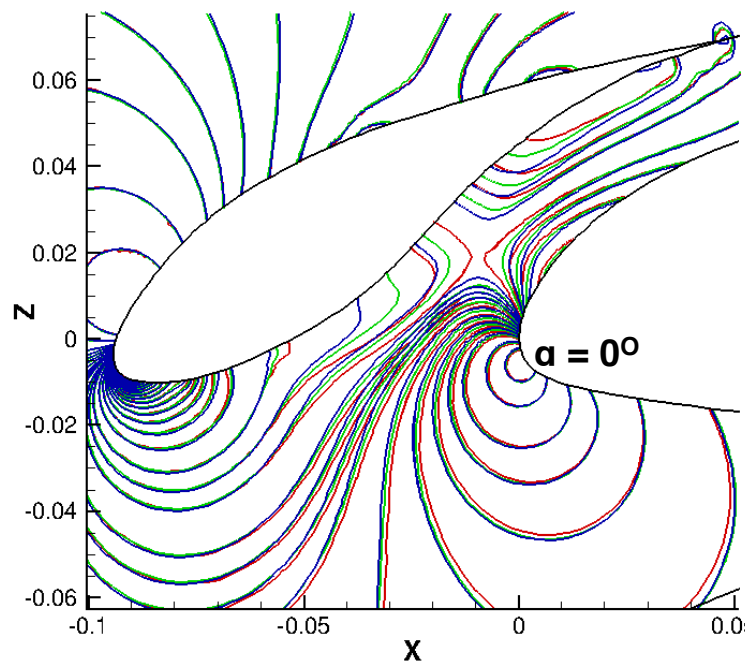
**Verification of CRWENO5 scheme with non-compact MUSCL3 and WENO5 schemes**



# SC2110 Airfoil w/ Slat in Wind Tunnel



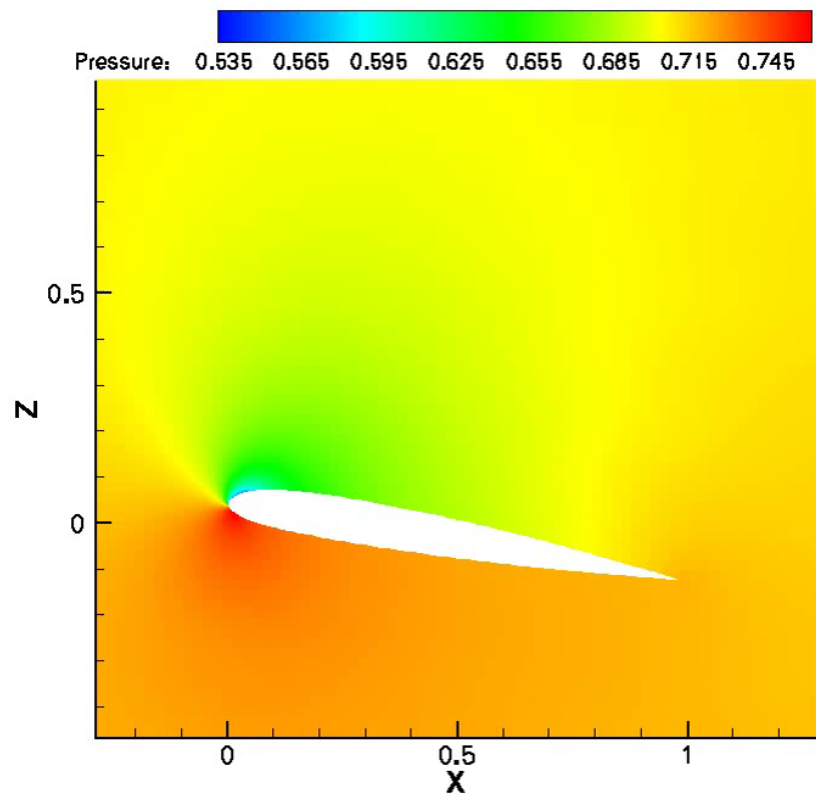
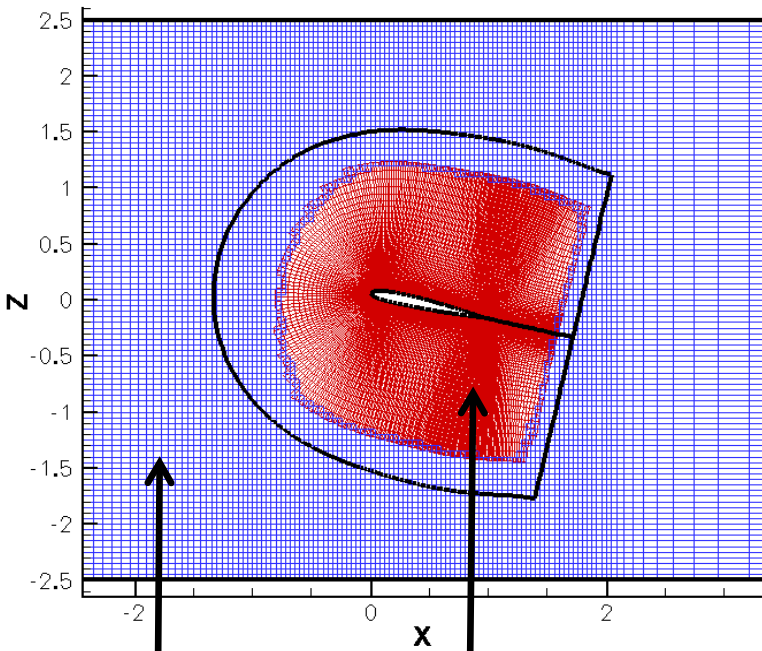
- High gradients in flow between slat and airfoil
- Overlap and solution transfer between slat and airfoil meshes
- Pressure contours from CRWENO5 compared with those from non-compact schemes



MUSCL  
WENO5  
CRWENO



# SC1095 Dynamic Stall



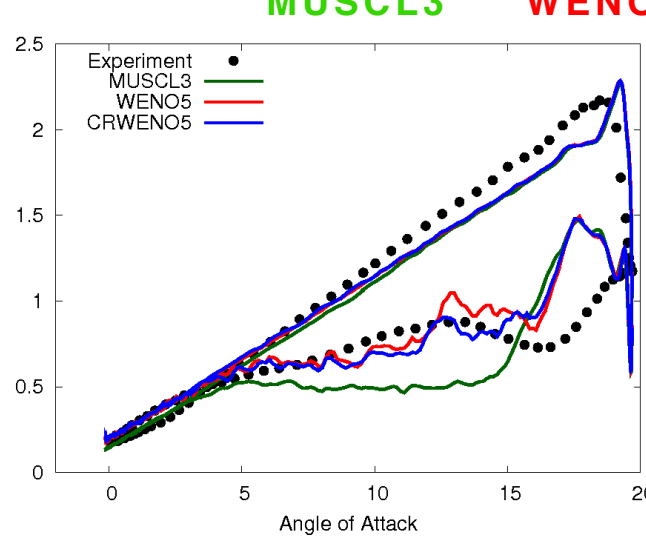
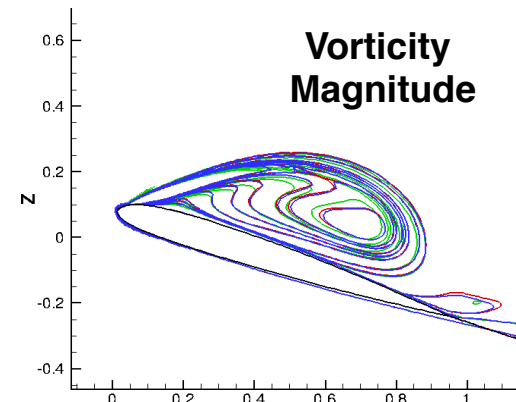
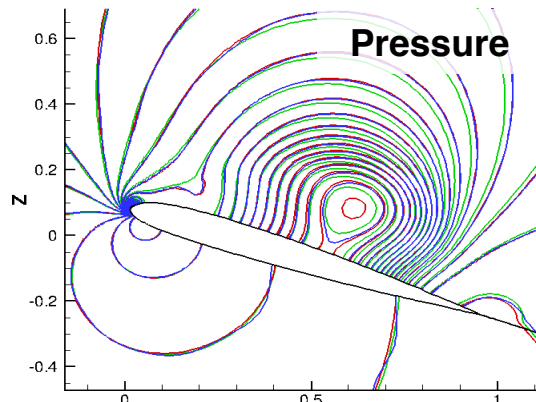
Wind Tunnel Mesh –  
Clustered Cartesian,  
151x101 points

**Flow Conditions:**  
Reynolds number: 3.92 million, Freestream Mach number 0.302  
Mean angle of attack: 9.78°, Pitch Amplitude: 9.9°, Reduced Frequency: 0.099, Tunnel height: 5c

**Numerical Solution:** Time stepping: BDF2 w/ 15 sub-iterations

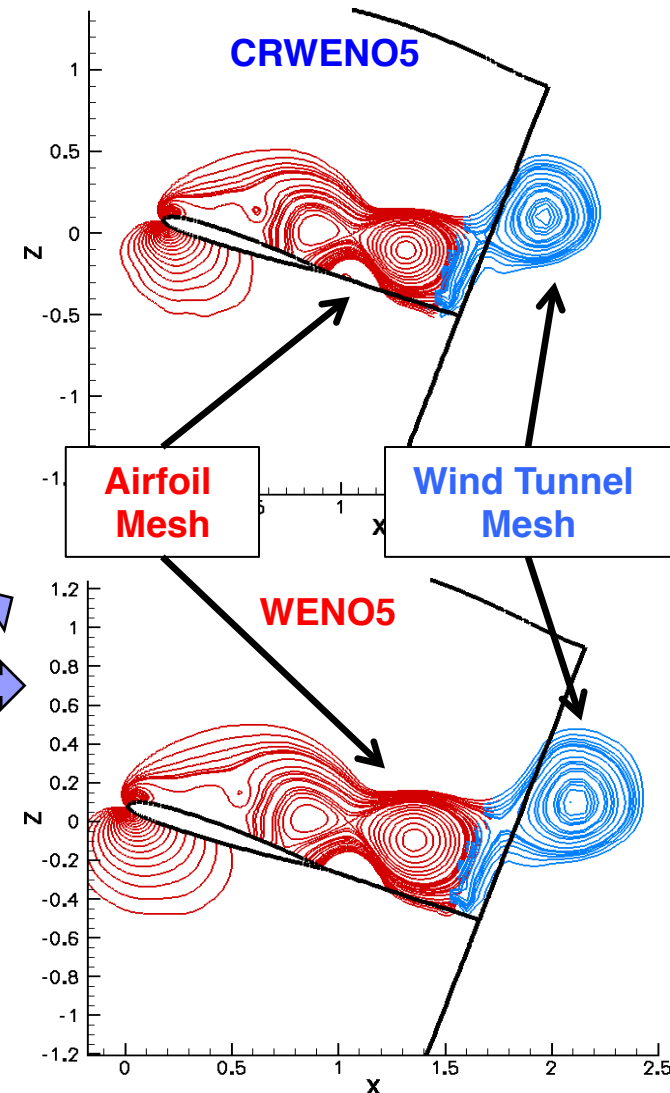
# SC1095 Dynamic Stall

## Validation for Overset Meshes w/ Grid Motion

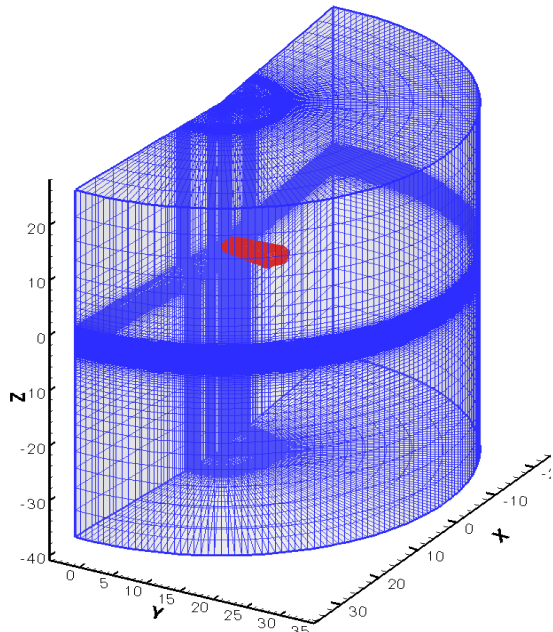


Shed vortices from upper surface

- Contour lines are continuous between airfoil and wind tunnel meshes
- Shed vortices pass smoothly between the two domains



# Harrington 2-Bladed Rotor

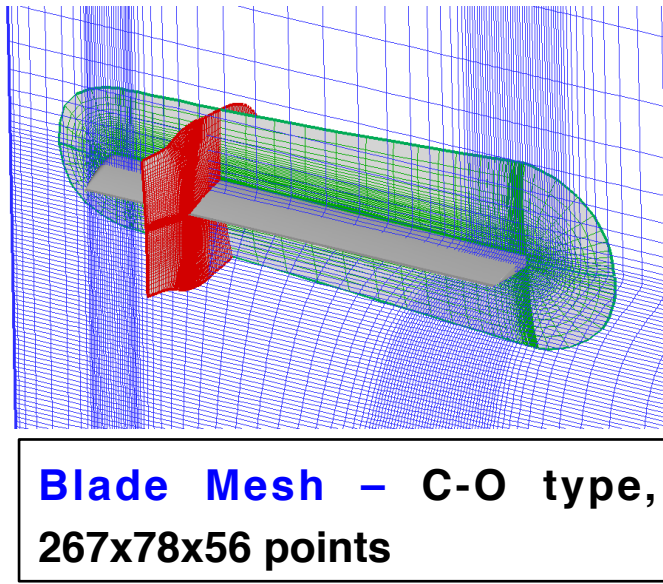


**Cylindrical Back-ground Mesh**  
**127 x 116 x 118 points**

**Rotor Geometry:**

- Aspect Ratio – 8.33
- Airfoil section – NACA

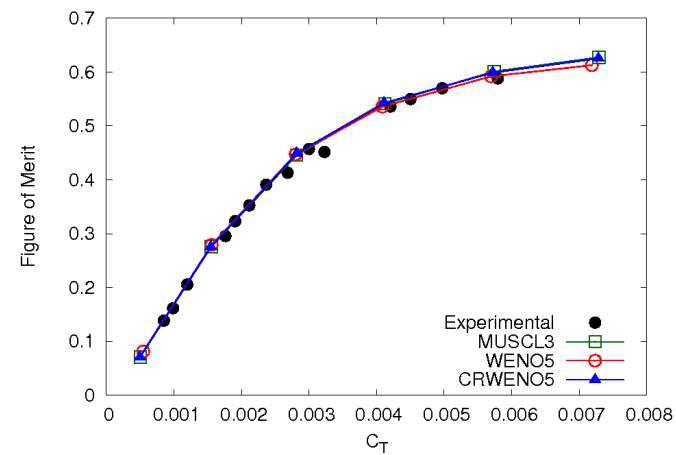
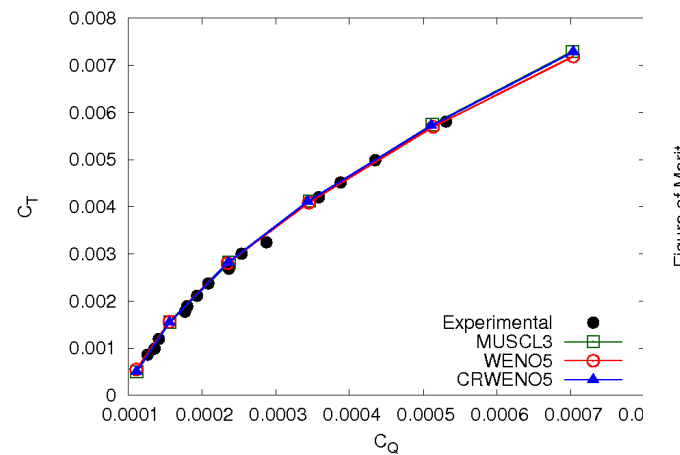
(t/c: 27.5% @ 0.2R, 15% @ R)



**Flow Conditions:**

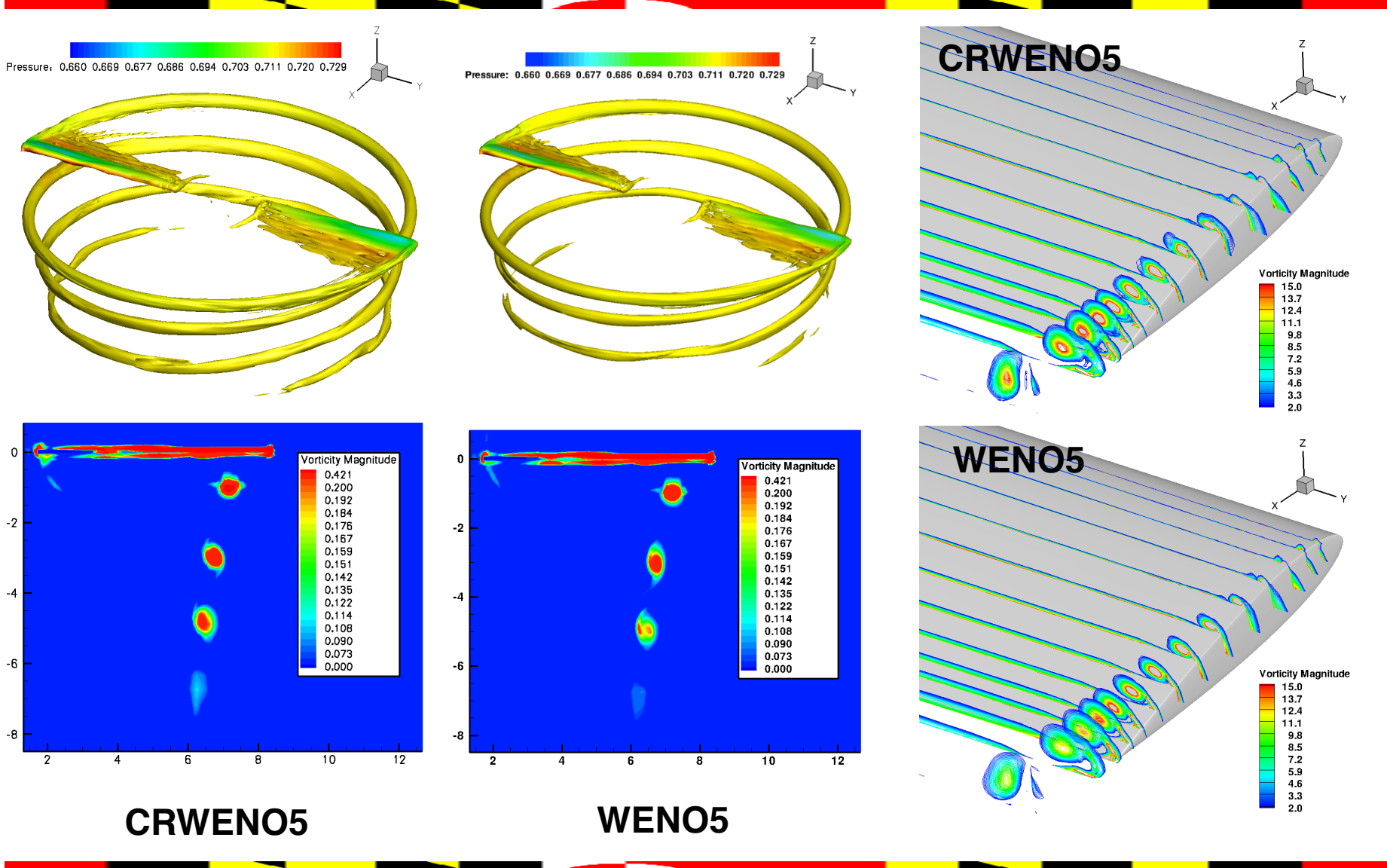
- $M_{tip}$ : 0.352
- $Re_{tip}$ : 3.5 million

**Validation of thrust & power coefficients and figure of merit**





# Harrington 2-Bladed Rotor (Near-Blade and Wake Flowfield)

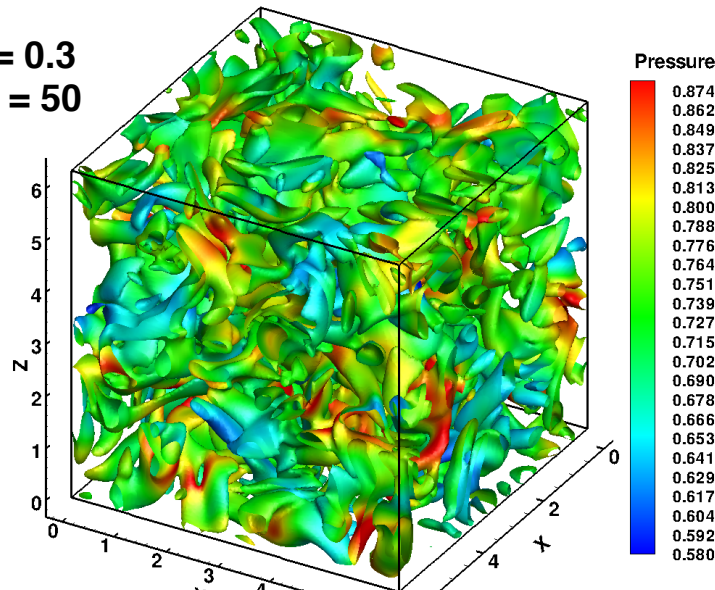


**CRWENO5**

**WENO5**

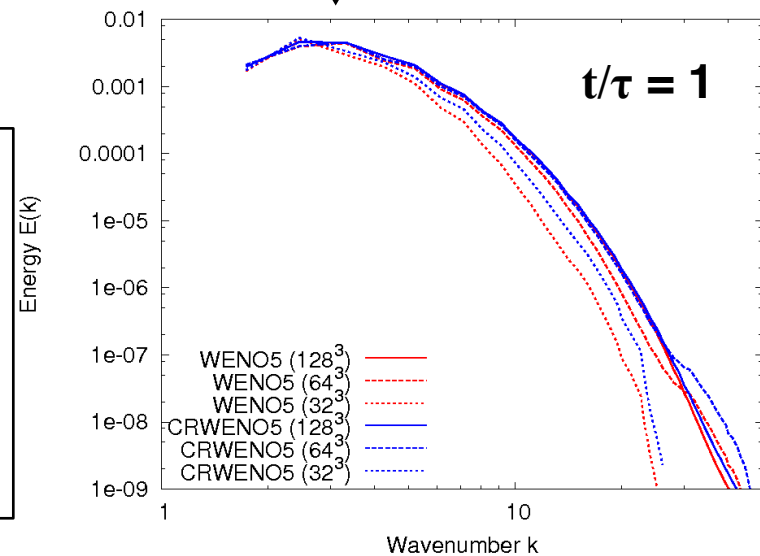
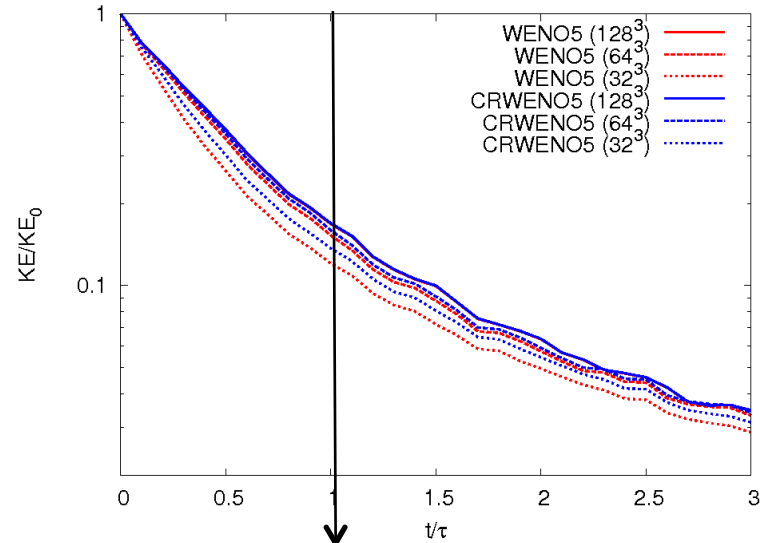
# Decay of Isotropic Turbulence

$M_t = 0.3$   
 $Re_\lambda = 50$

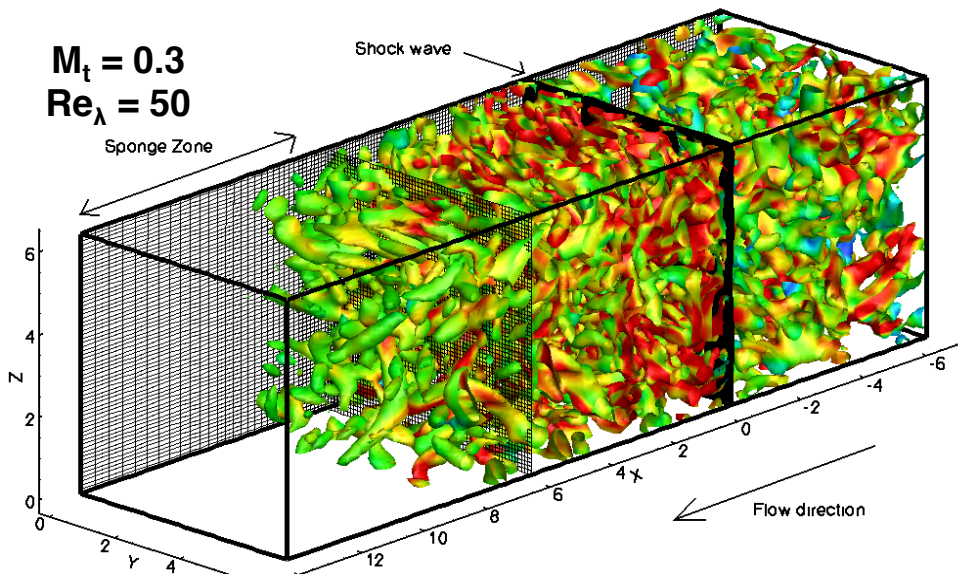


Iso-surfaces of vorticity magnitude, colored by pressure

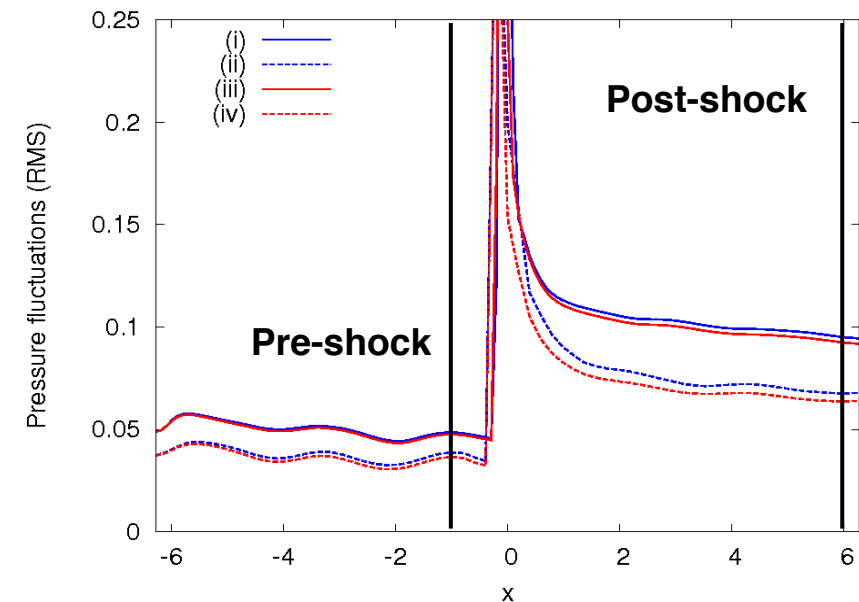
- Flow involves energy transfer to smaller length scales
- Grid-converged solutions obtained on  $128^3$  grid (WENO5 & CRWENO5 agree)
- CRWENO5 shows better resolution of intermediate and higher wavenumbers



# Shock – Turbulence Interaction



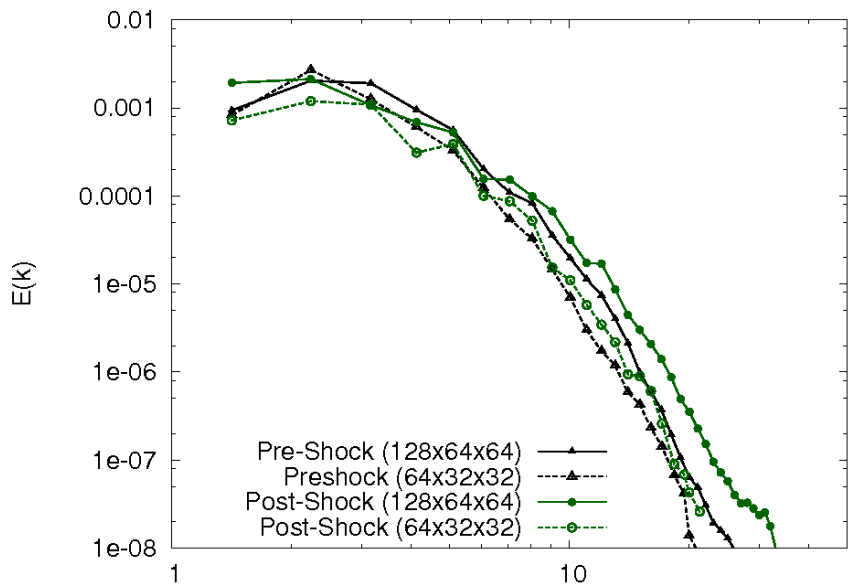
Iso-surfaces of 2<sup>nd</sup> invariant of velocity tensor,  
colored by vorticity magnitude



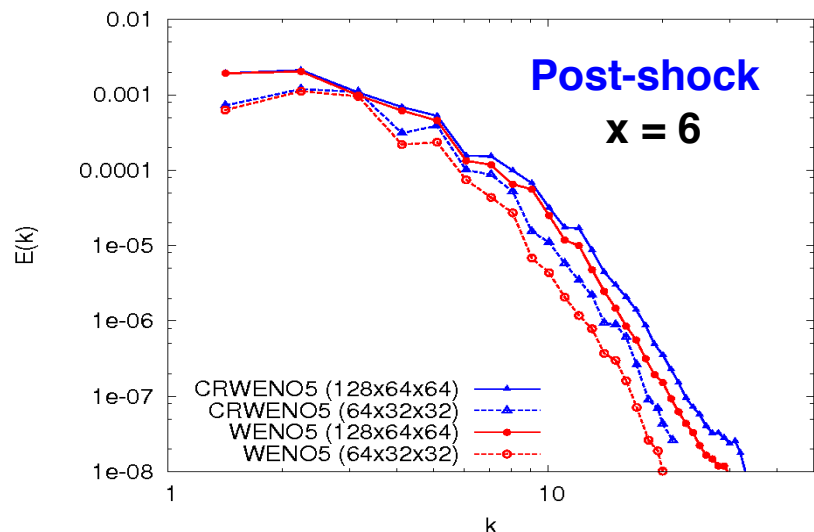
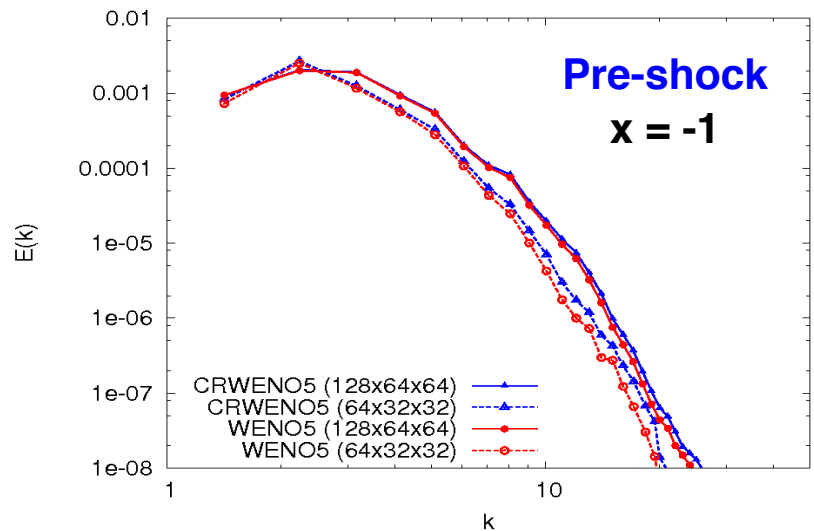
Stream-wise pressure fluctuations (RMS)

- Inflow: Fluctuations from isotropic turbulence decay added to mean flow at Mach 2
- Interaction with a shock wave **magnifies the turbulent fluctuations**
- Problem solved on two grids: 64x32x32 and 128x64x64 points (uniform)
- CRWENO5 → Lower dissipation → **Predicts higher levels of fluctuations** on both grids

# Shock – Turbulence Interaction



- Interaction with a shock wave amplifies intermediate and higher wavenumbers
- CRWENO5 shows improved resolution of the smaller length scales (for both grids)





# Conclusions and Future Work

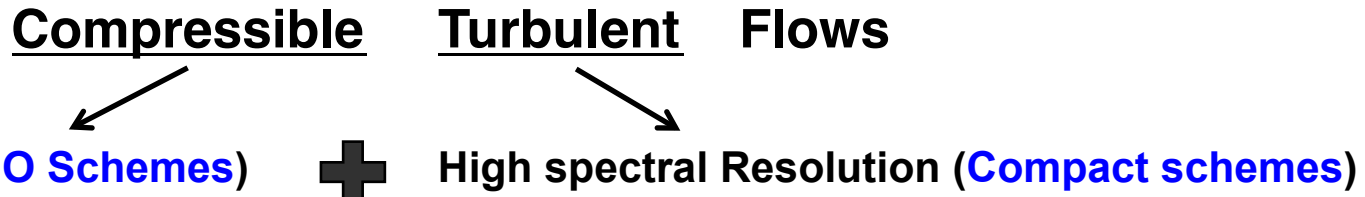


# Conclusions

- **Derivation and implementation of 5<sup>th</sup> order CRWENO schemes**
  - Higher accuracy: Lower absolute errors than 5<sup>th</sup> order WENO scheme
  - Reduced clipping and smearing for discontinuities and extrema
  - Higher computational efficiency: Lower runtime than the WENO scheme for solutions with same accuracy and resolution
- **Extension to system of equations: inviscid Euler equations**
  - Implemented for reconstruction of conserved, primitive & characteristic variables
  - Higher accuracy and reduced smearing & clipping of discontinuities
  - Improved resolution of small-length scale waves (Shock-entropy wave interaction)
  - Improved preservation of vortex strength and shape (Isentropic vortex convection)
  - Higher computational efficiency for conserved/primitive reconstruction, NOT for characteristic based reconstruction
- **Integration with a finite-volume Navier-Stokes solver**
  - Applied to steady/unsteady flow past airfoils / wing / rotor
  - Validated for curvilinear grids + overset meshes with relative motion
  - Improved resolution of near-blade and wake flow features (vortical structures)
  - DNS of compressible turbulent flows: Lower dissipation of smaller length scales



# Key Contributions



## Introduction of the Compact-Reconstruction WENO scheme

- Applies the WENO algorithm (solution-dependent interpolation) to compact schemes
- **High spectral resolution** → Improved resolution of small length scales
- **Non-oscillatory interpolation** across discontinuities and steep gradients
- **Higher accuracy** → Preservation of flow features for long-term convection
- **Applicable to overset meshes** with no special treatment

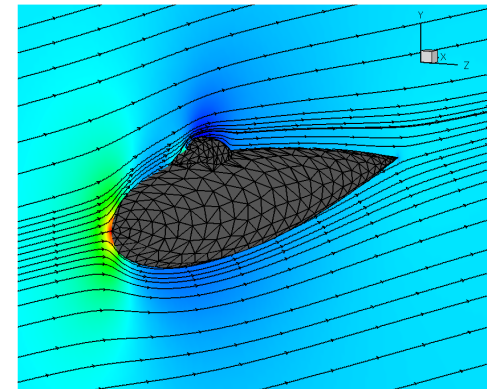
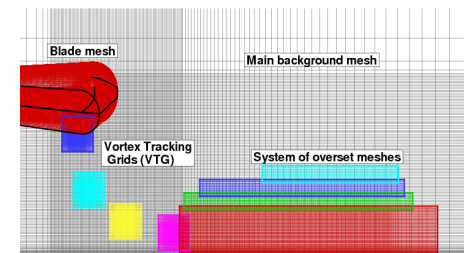
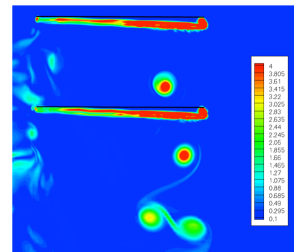
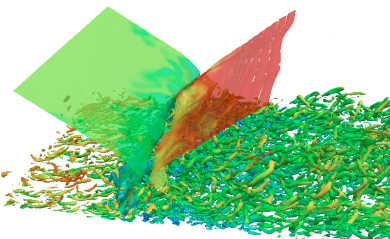
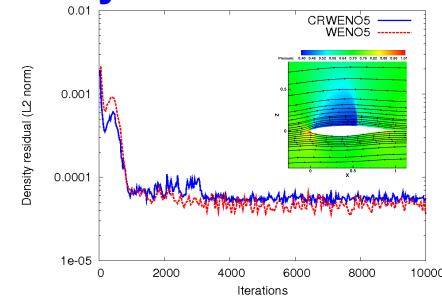


## Comparison with compact-WENO hybrid schemes

- No need for an additional switching parameter
- Does not revert to non-compact scheme (poor spectral resolution) near discontinuities

# Future Work

- Improvements / extensions of the numerical scheme
  - Implementation of non-linear weights (convergence for stationary shock and steady flow around airfoils)
  - Derivation for non-uniform grids
  - Implementation of a 9<sup>th</sup> order CRWENO scheme
  - Fine & medium grain parallelization issues
  - Use of monotonicity-preserving (MP) limits (Suresh & Huynh, 1997)
- Applications
  - High – resolution solutions to aircraft / rotorcraft wake flow and interaction with ground plane for rotorcraft operating IGE
  - Implementation for domains with immersed boundaries
  - DNS of shock – boundary layer interactions





# Acknowledgments

This research was supported by the **U.S. Army's MAST CTA Center for Microsystem Mechanics** with Mr. Chris Kroninger (ARL-VTD) as Technical Monitor.

<http://www.mast-cta.org/>